Journal of The Electrochemical Society

OPEN ACCESS

Review—Recent Developments in the Applications of 2D Transition Metal Dichalcogenides as Electrocatalysts in the Generation of Hydrogen for Renewable Energy Conversion

To cite this article: Ramaraj Sukanya *et al* 2022 *J. Electrochem. Soc.* **169** 064504

Journal of The Electrochemical Society, 2022 **169** 064504

Review—Recent Developments in the Applications of 2D Transition Metal Dichalcogenides as Electrocatalysts in the Generation of Hydrogen for Renewable Energy Conversion

Ramaraj Sukanya,[1] Daniele C. da Silva Alves,[1] and Carmel B. Breslin[1,2,*,z]

[1]*Department of Chemistry, Maynooth University, Maynooth, Co. Kildare, Ireland*
[2]*Kathleen Lonsdale Institute for Human Health Research, Maynooth University, Maynooth, Co. Kildare, Ireland*

There has never been a more pressing need to develop sustainable energy systems as dramatic climate changes emerge across the World. Some of these effects can be alleviated by the development of efficient devices that are capable of producing hydrogen gas in an environmentally acceptable manner, which in turn can be employed as a clean fuel. In this context, the splitting of water is especially attractive. However, this technology requires the design of new cost-effective electrocatalytic materials. In this review, the progress made in the development of transition metal dichalcogenides (TMDs) and their composites as electrocatalysts for both acidic and alkaline electrolysis cells and as photocatalysts for the formation of hydrogen is described and discussed. Following a short introduction to the mechanisms of the electrochemical hydrogen and oxygen evolution reactions and the photoelectrochemical generation of hydrogen, an introduction to TMDs, their relevant general properties and the methods used in their synthesis are described. Then, the performance of various TMD-based materials in the electrochemical splitting of water is discussed, with a final brief overview of the application of TMDs in photoelectrochemical devices. Although challenges clearly remain, TMD-based materials are emerging as promising electrocatalysts and photoelectrocatalysts for the production of hydrogen.
 [DOI: 10.1149/1945-7111/ac7172]

Manuscript submitted January 14, 2022; revised manuscript received May 12, 2022. Published June 6, 2022. *This paper is part of the JES Focus Issue on Advanced Electrolysis for Renewable Energy Storage.*

The recent 26th UN climate change conference of the parties "(COP26)" which was held in the UK in "2021" highlighted the ever pressing need to reduce and eliminate the burning of fossil fuels. The combustion of fossil fuels gives rise to the production of carbon dioxide and other greenhouse gases, which are particularly harmful to the environment, resulting in ozone depletion, global warming, acid rain, and many other detrimental effects.[1–3] As these greenhouse gases continue to accumulate in the atmosphere, dramatic changes are emerging in the Earth's Climate.[4]

Clearly, a transition to an affordable and sustainable energy system is urgently required and this can only be achieved by investing in renewable energy resources, prioritising energy efficient practices, and adopting clean energy technologies. Hydrogen is widely regarded as a promising energy carrier and has the capacity to fulfil our energy needs cleanly and sustainably.[5] In particular, hydrogen is a lightweight molecule with a high energy density, higher than that of any fossil fuel. It is a sustainable, eco-friendly, and non-toxic energy carrier with water as a by-product when combined with oxygen, and as a fuel it releases no harmful gases. With the increasing interest in generating hydrogen using environmentally acceptable approaches, there has been a renewed interest in the well-known electrochemical splitting of water into hydrogen and oxygen, which is now considered as one of the more promising approaches in the generation of hydrogen.[6,7] This reaction is achieved by two half-cell reactions in an electrochemical cell: the hydrogen evolution reaction (HER) at the cathode, and the oxygen evolution reaction (OER) at the anode. In this approach, the excess energy from renewable energy sources can be used to facilitate the splitting of water, thereby converting this excess energy, that otherwise may be lost, into molecular hydrogen, a clean fuel.[7,8] Since these renewable energy sources are intermittent, the stored hydrogen (green or renewable hydrogen) can be used as a fuel in fuel cell applications, providing energy when needed.

However, energy and electrocatalysts are required to promote the water splitting reaction, as the electrolysis of water is not a thermodynamically viable process. Currently, the most efficient electrocatalysts are precious noble metals, such as Pt-based,[9,10] and to a lesser extent Ru-based materials,[11] for the HER (in both proton exchange membrane cells (PEM) and alkaline cells). Indeed, platinum exhibits a very low overpotential for the evolution of hydrogen, making it the most efficient electrocatalyst for HER. Precious Ir/Ru-based materials are very efficient in promoting the OER.[12,13] However, the high cost and scarcity of these precious metals limits their wide spread and large scale applications. Single atom electrocatalysts have been investigated extensively[14,15] with the aim of reducing to a minimum the amount of the expensive metal component. Good electrocatalytic HER performances have been obtained with single atom Pt,[16] Ru,[17,18] Pd,[19] Co,[20] Mo,[21] Fe,[22] Ni,[23] and W.[24] However, these single metal atom electrocatalysts are prone to aggregation, due to the large surface energy of the single metal atoms, limiting their overall stability, while interactions with the support materials can be complex and are not fully understood.

Another approach is to develop non-precious metal-based electrocatalysts, eliminating the need to use Pt and Ru based materials. In recent years, there has been considerable focus on identifying earth-abundant materials that have the potential to match the performance of the precious metal-based electrocatalysts. In particular, transition metal (TM) based electrocatalysts, including carbides,[25,26] nitrides,[26,27] borides,[28,29] phosphides,[30] layered double hydroxides[31,32] and transition metal dichalcogenides (TMDs)[33–36] are now attracting significant attention. Also, metal-free carbon-based materials,[37] such as graphene[38,39] and carbon nanotubes,[40] have emerged as promising and low-cost electrocatalysts for water splitting. Among all these materials, TMDs are rapidly emerging as alternative cost-effective electrocatalysts for the platinum-based systems.[34,41] This is not surprising as these materials, especially the disulfides[41,42] and diselenides,[42,43] have a unique set of interesting physicochemical properties and can be readily doped with a variety of TMs[36,43,44] to further enhance their catalytic activity. When exfoliated into a few 2D layers, they not only exhibit very good electrocatalytic activity for the production of $H_2(g)$[45,46] and indeed the evolution of $O_2(g)$,[47] but also a very impressive photocatalytic activity for the solar water splitting reaction.[48–50]

In this review, the applications of TMD-based materials as electrocatalysts and photoelectrocatalysts for the generation of hydrogen through the splitting of water are reviewed. Although there are a number of excellent review articles that describe the synthesis and properties of TMDs[51,52] and their applications in the

*Electrochemical Society Member.
[z]E-mail: Carmel.Breslin@nuim.ie

energy sector,[53–55] we focus on the emerging applications of TMDs in the electrochemical production of hydrogen. Initially, we describe the overall mechanisms of the HER, OER and photoelectrochemical formation of hydrogen, the relevant properties of TMDs and a summary of the main methods employed in their synthesis. Next, we review and discuss the emerging applications of TMD-based electrocatalysts in water splitting, including the various companion materials used in the formation of the TMD-based hybrids, composites and semiconductor heterojunctions. Finally, the challenges that remain to be resolved before TMD-based electrocatalysts can be employed in the design of electrochemical and photoelectrochemical devices for the production of hydrogen are discussed.

Electrolysis and Photo-Assisted Splitting of Water

As detailed earlier the splitting of water involves two half-reactions, the HER, Eq. 1, which occurs at the cathode, and the OER, Eq. 2, which takes place at the anode in the electrochemical cell. These two redox reactions have been studied extensively. It is now generally accepted that the HER proceeds with the initial adsorption of a hydrogen atom, either through the Volmer–Heyrovsky or the Volmer–Tafel mechanisms.[56,57] Depending on the pH of the solution, the reduction of protons or water molecules occurs to give adsorbed hydrogen atoms on the surface of the metal or catalyst (*M–H), where * represents an active adsorption site on the electrocatalyst (M). This first adsorption step is known as the Volmer reaction and this is illustrated for acidic media in Eq. 3 and for basic environments in Eq. 4.

$$2H^+(aq) + 2e^- \rightarrow H_2(g) \quad [1]$$

$$2H_2O(l) \rightarrow O_2(g) + 4H^+(aq) + 4e^- \quad [2]$$

$$H^+(aq) + e^- + {}^*M \rightarrow {}^*M - H \quad [3]$$

$$H_2O(l) + e^- + {}^*M \rightarrow {}^*M - H + OH^-(aq) \quad [4]$$

Depending on the nature of the electrode and/or the electrocatalyst, the $H_2(g)$ can then be formed through the combination of two adsorbed hydrogen atoms (Tafel reaction), Eq. 5. Alternatively, in accordance with the Heyrovsky reaction, the adsorbed hydrogen atom may combine with an electron and a proton or water molecule, Eqs. 6 (acidic) and 7 (basic), to give the generation of $H_2(g)$. In many cases, the Volmer reaction becomes the rate-determining step and for non-precious metal-based electrocatalysts, such as the dichalcogenides, the reaction proceeds mainly with the Volmer followed by the Heyrovsky reaction, to give the Volmer–Heyrovsky mechanism. The pH of the electrolyte can also have a significant effect on the rate of the HER reaction. As illustrated in Eq. 4, water adsorption plays a crucial role in the Volmer reaction in alkaline media and in this case, the electrocatalysts must facilitate the adsorption of water, water dissociation and hydrogen binding. Normally, high overpotentials are required in alkaline solutions due to the sluggish kinetics of the HER and this remains a challenge in the development of active and stable HER electrocatalysts in alkaline media.[58]

$${}^*M - H + {}^*M - H \rightarrow {}^*M + {}^*M + H_2(g) \quad [5]$$

$${}^*M - H + H^+(aq) + e^- \rightarrow {}^*M + H_2(g) \quad [6]$$

$${}^*M - H + H_2O(l) + e^- \rightarrow {}^*M + OH^-(aq) + H_2(g) \quad [7]$$

The OER is an equally important half-reaction in the electrolysis of water and this reaction can be summarised in Eq. 8 for acidic solutions and in Eq. 9 for basic media. This reaction, which involves the transfer of four protons coupled with four electrons and bond breakage and formation, is more complex, and kinetically sluggish compared with the HER. Indeed, the overall efficiency of the electrocatalytic water splitting reaction in an electrolysis cell is usually limited by the OER. The standard reduction potential, E^o, for the OER is 1.23 V vs SHE, however much higher applied potentials are needed for the production of $O_2(g)$, resulting in high overpotentials. While the mechanism of the OER is complex and strongly dependent on the nature of the electrocatalyst, the most widely recognised OER mechanism is the adsorbate evolution mechanism (AEM). In this case, the first step in an alkaline electrolyte is the adsorption of $OH^-(aq)$ at an adsorption site (*M), to give the adsorbed ${}^*M–OH$ species, Eq. 10. The *M–OH intermediates then further combine with $OH^-(aq)$ to give the formation of $H_2O(l)$ and adsorbed *M–O atoms, Eq. 11. This is followed by the formation of adsorbed *M–OOH, Eq. 12, which then reacts with additional $OH^-(aq)$ to give $O_2(g)$ and $H_2O(l)$, Eq. 13.

$$2H_2O(l) \rightarrow 4H^+(aq) + O_2(g) + 4e^- \quad [8]$$

$$4OH^-(aq) \rightarrow 2H_2O(l) + O_2(g) + 4\,e^- E^0/V \text{ vs SHE} = 1.23 - 0.059(\text{pH}) \quad [9]$$

$${}^*M + OH^-(aq) \rightarrow {}^*M - OH + e^- \quad [10]$$

$${}^*M - OH + OH^-(aq) \rightarrow {}^*MO + H_2O(l) + e^- \quad [11]$$

$${}^*M - O + OH^-(aq) \rightarrow {}^*M - OOH + e^- \quad [12]$$

$${}^*M - OOH + OH^-(aq) \rightarrow {}^*M + O_2(g) + H_2O(l) + e^- \quad [13]$$

In addition to fresh water, there is now increasing interest in employing seawater as the electrolyte in the electrolysis cell as it provides an unlimited eco-friendly resource.[59,60] However, the presence of high concentrations of chloride (approximately 0.5 M in seawater), and the associated chloride oxidation reaction to yield $Cl_2(g)$ under acidic conditions, Eq. 14, and hypochlorite at the anode in more alkaline solutions, Eq. 15, present a major challenge. These oxidation reactions can compete with the OER. The OER is more thermodynamically favourable than the oxidation of the chloride anion, irrespective of the pH of the solution phase. For example, in alkaline solutions, the equilibrium potential of the OER is lower by about 490 mV compared with the oxidation of the chloride anion. However, high overpotentials are required to promote the OER, while the oxidation of chloride anions is a more facile two-electron oxidation reaction with a kinetic advantage. Normally, the evolution of chlorine, Eq. 14, is the predominant reaction in acidic chloride-containing aqueous solutions. Although the formation of hypochlorite, Eq. 15, has a kinetic advantage over the evolution of oxygen, the OER has been achieved in alkaline seawater solutions.[59] Furthermore, the chloride anion is well known to promote the corrosion of a wide range of metal-based materials[61] and this can have a significant effect on the longer term performance of the electrocatalysts when employed in seawater. Therefore, the development of electrocatalysts that have good stability in the presence of high concentrations of chloride anions coupled with selectivity for the OER are essential for practical applications in seawater electrolysis.

$$2Cl^-(aq) \rightarrow Cl_2(g) + 2e^- \; E^0/\text{V vs SHE} = 1.36 \text{ V} \quad [14]$$

$$Cl^-(aq) + 2OH^-(aq) \rightarrow OCl^-(aq) + 2H_2O(l) + 2e^- \; E^0/\text{V vs SHE} = 1.72 - 0.059(\text{pH}) \quad [15]$$

Another approach that has received considerable attention is the use of light with semiconductors to generate electron (e^-) and hole (h^+) pairs that facilitate the reduction of water to give $H_2(g)$ and the oxidation of OH^- ions or H_2O to give $O_2(g)$, Fig. 1a. Ever since the

pioneering work of Honda and Fujishima in 1972, where a photoelectrochemical cell consisting of TiO_2 as the semiconductor anode and platinum as the counter electrode under UV irradiation and electrochemical bias was employed to split water,[62] there has been significant focus on finding more efficient and high performing semiconducting materials. Typically, photoelectrochemical (PEC) splitting of water consists of a semiconductor photoanode and a metal cathode Fig. 1b, a semiconductor cathode and a counter electrode, Fig. 1c, or a semiconductor anode and cathode, Fig. 1d. As illustrated in Fig. 1b, an electron is promoted from the valence band to the conductance band on the absorption of photons that have sufficient energy to match the bandgap energy. This results in the generation of a h^+ in the valence band and an e^- in the conduction band. The e^- can flow to the cathode where the reduction of water occurs to give $H_2(g)$ and this separation of charge minimises the e^-/h^+ recombination reaction. Provided the h^+ resides in a sufficiently low energy level to make the oxidation of OH^- a thermodynamically feasible reaction, the h^+ can facilitate the oxidation event, and in the process generate $O_2(g)$. There is also considerable interest in the use of hybrid photovoltaic–photoelectrochemical (PV–PEC) systems,[63,64] where the production of $H_2(g)$ arises from the coupling of a photovoltaic solar cell with a water electrolysis system. In each of these approaches, the properties of the semiconductor are important. Much focus is placed on the design of earth abundant and metal free semiconductors with good stability and durability that are capable of harnessing light in the visible region and that are cost-effective.[65–67] Considering all the different materials that are potentially promising as electrocatalysts for the splitting of water, acting as HER and OER electrocatalysts and furthermore as semiconductors for the photocatalytic splitting of water, TMDs are emerging as promising materials. As will become evident in the following sections, the synthesis of TMDs can be carried out with relative ease, the TMDs can be exfoliated, they can be easily combined with other materials and have a bright future in the electrochemical splitting and photoelectrocatalytic splitting of water.

Introduction to Transition Metal Dichalcogenides (TMDs)

Since the discovery of graphene, various new 2D materials have been discovered or rediscovered,[68–71] and among these, TMDs are emerging as intriguing and efficient electrocatalytic layered materials with high surface areas and good chemical stability.[69–71] The TMDs can not only promote the electrolysis of water, but have interesting semiconducting properties, that can be tuned and exploited in PEC cells. This ability to form TMDs with a range of conductivities, spanning from semiconductors[70,71] to metallic-like conduction and superconductors,[72] means that they can be tailored for a range of different applications. The TMDs can be represented as MX_2, where M is a transition metal, belonging to group IV–IX, (typically Mo, W, V, Re, Ta, Ti) and X is a chalcogen atom, S, Se or Te. The M atoms are arranged in a lattice and are sandwiched between two chalcogen atoms, as illustrated in Fig. 2a, to give X–M–X. Covalent bonding exists between the M and X atoms, while the layers are stacked, with the adjacent layers being held by weak van der Waals forces.

In terms of crystal phases, the TMDs can exhibit different phases, with the two main heterogeneous polymorphic structures being the octahedral coordination phase (1T), which shows metallic-like properties, and the trigonal prismatic phase (2H), which gives

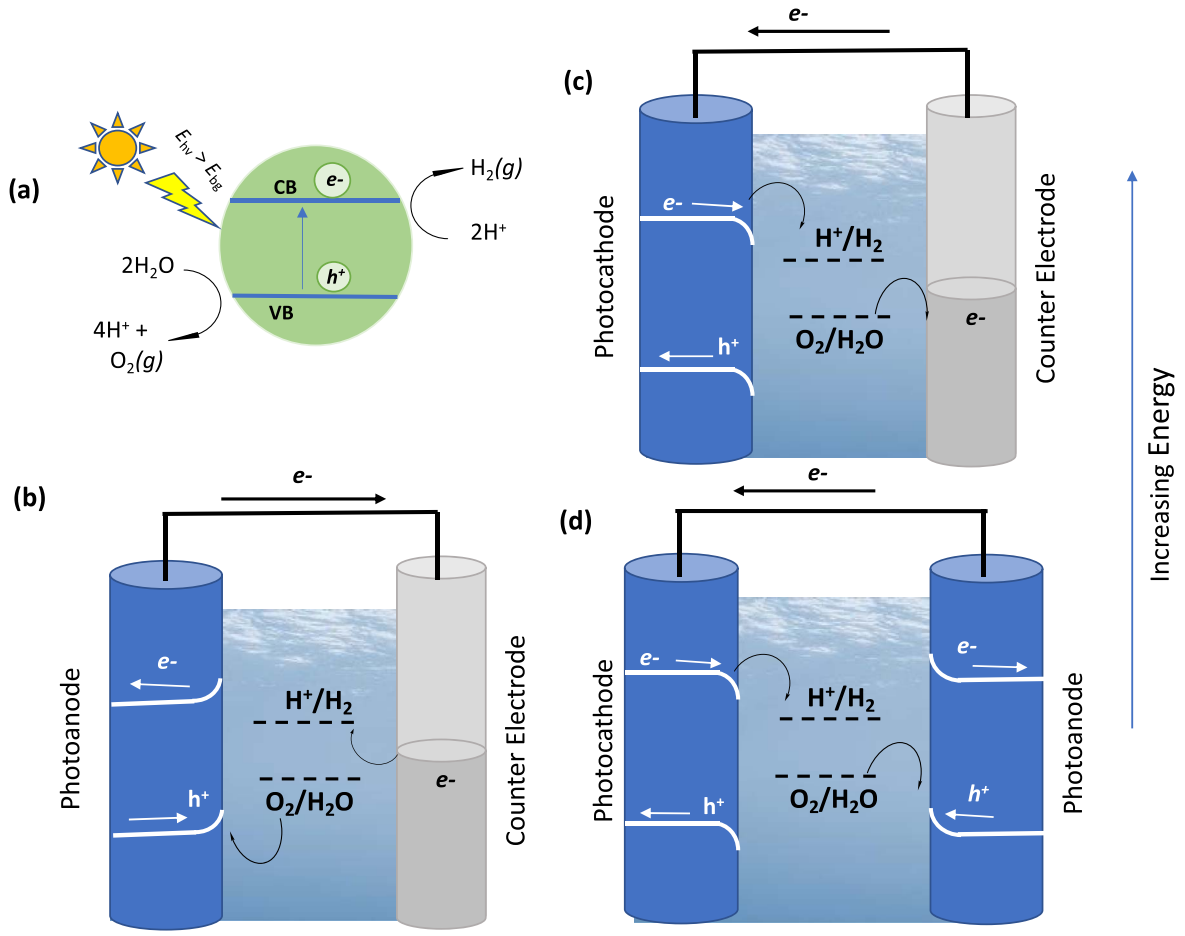

Figure 1. Schematic representation of (a) generation of e^-/h^+ at an semiconductor on absorption of a photon of light, sufficient to match the bandgap energy, and electron-transfer reactions on activation of a (b) photoanode and (c) photocathode coupled with counter electrodes, and (d) a photocathode coupled with a photoanode, where the E^o/SHE of $H^+/H_2(g)$ is 0 V and E^o/SHE of $O_2(g)/H_2O$ is 1.23 V, under acidic conditions (pH = 0).

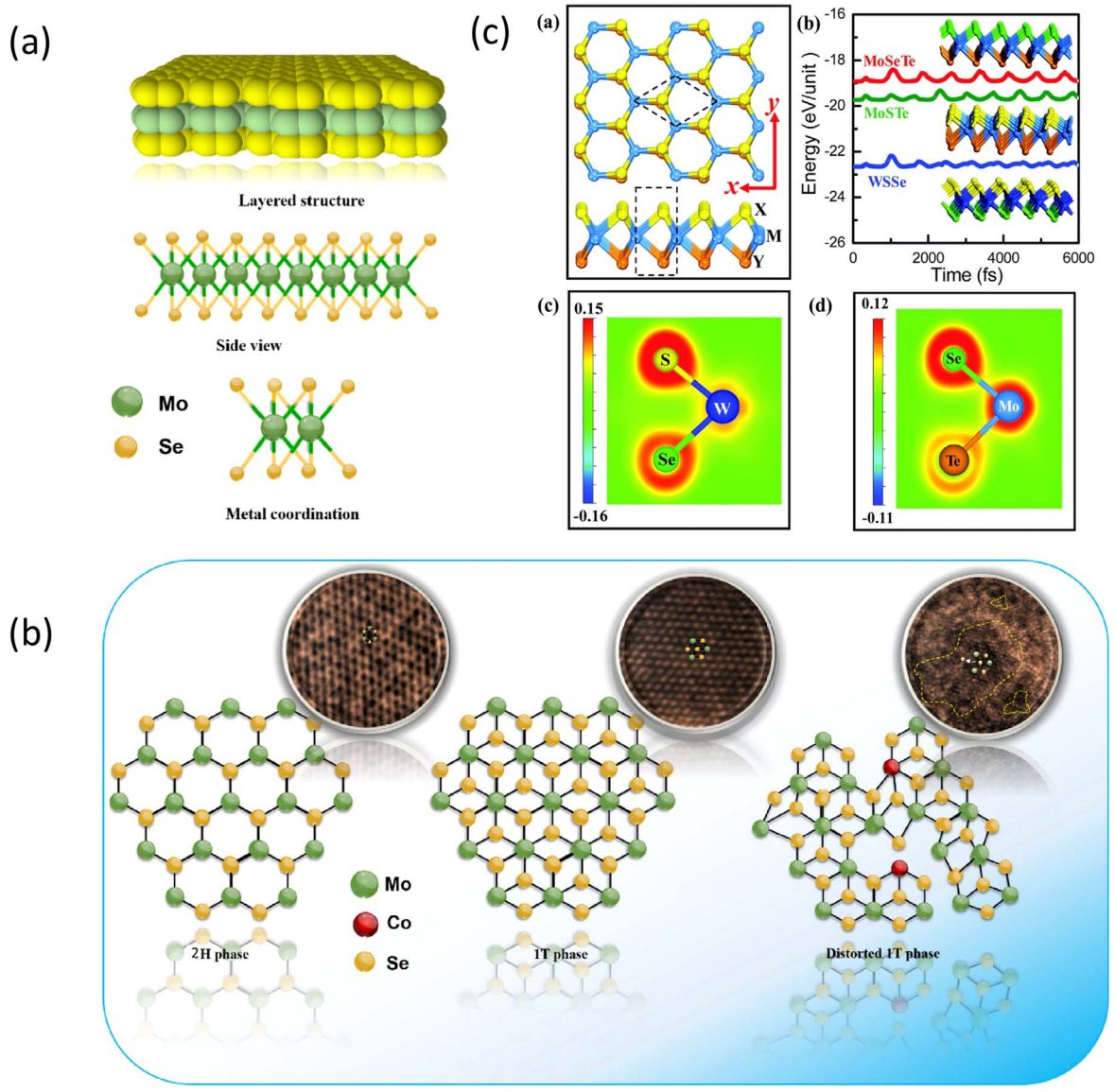

Figure 2. Schematic representation of (a) $MoSe_2$ (MX_2), (b) Different polymorphism of $MoSe_2$ reproduced with permission from S. Ramaraj et al.[73] Copyright 2019 American Chemical Society (c) representation of the Janus TMDs reproduced with permission from Wang et al.[66] Copyright 2018 Royal Society of Chemistry.

semiconductor-like properties. A third distorted octahedral (1T' phase) phase can also be observed and this phase has semi-metallic characteristics.[74] These are schematically illustrated in Fig. 2b. The 1T phase has a low charge transfer resistance and improved electrocatalytic activity, making it a very interesting material for electrochemical applications.[75] The 2H phase is normally the thermodynamically favoured phase. However, it has been shown that some family members naturally crystalise in the 1T or 1T' phases.[76] One of the more popular methods used in the conversion of the 2H to the 1T phase involves solution phase intercalation, where the intercalated Li^+, Na^+ or K^+ facilitate charge transfer.[77–79] Ammonium ions, NH_4^+, have also been employed to stabilise the 1T phase,[80] while it has been shown that non-metal doping, for example with P, can also be used to promote the formation of the metallic 1T phase.[71]

In addition, it is well established that the basal plane is electrochemically inert, particularly in the case of the more well-known MoS_2, WS_2, $MoSe_2$ and WSe_2, and that the electrocatalytic activity arises from the edge sites.[81] Therefore, the introduction of strain or defects on the basal plane of these layered structures offers more active sites (kinks, terraces, corner atoms, chalcogenide and/or transition metal vacancies, point defects, and grain boundaries), which facilitate fast electron transfer.[82] Edge sites, distorted active sites and terrace sites are schematically shown in Fig. 3. Methods such as defect engineering, including exposure to an oxygen plasma, electron beam irradiation or heteroatom doping,[82,83] can all be employed to give a high density of active sites. Indeed, the creation of defects and distortions to give active sites on these layered structures has become an intense research topic in recent years with various transition metal doped TMDs emerging.[36,84,85]

Recently, there has been much interest and focus on asymmetric TMDs, which are described as Janus TMDs, with an asymmetric X–M–Y structure, such as SMoSe. In this case, as illustrated in the schematic in Fig. 2c, the transition metal layer is sandwiched between two different chalcogen layers and this gives rise to a reduction in structural symmetry, which in turn can lead to different electronic and optical properties. These Janus TMD layers are attracting considerable attention in both electrocatalysis[87,88] and photocatalysis.[89] In addition, TMD heterostructures are emerging as new materials with intriguing properties. In this case, different TMD monolayers are stacked to form heterostructures held by weak van der Waals forces, such as $MoSe_2/WS_2$.[90] These heterostructures

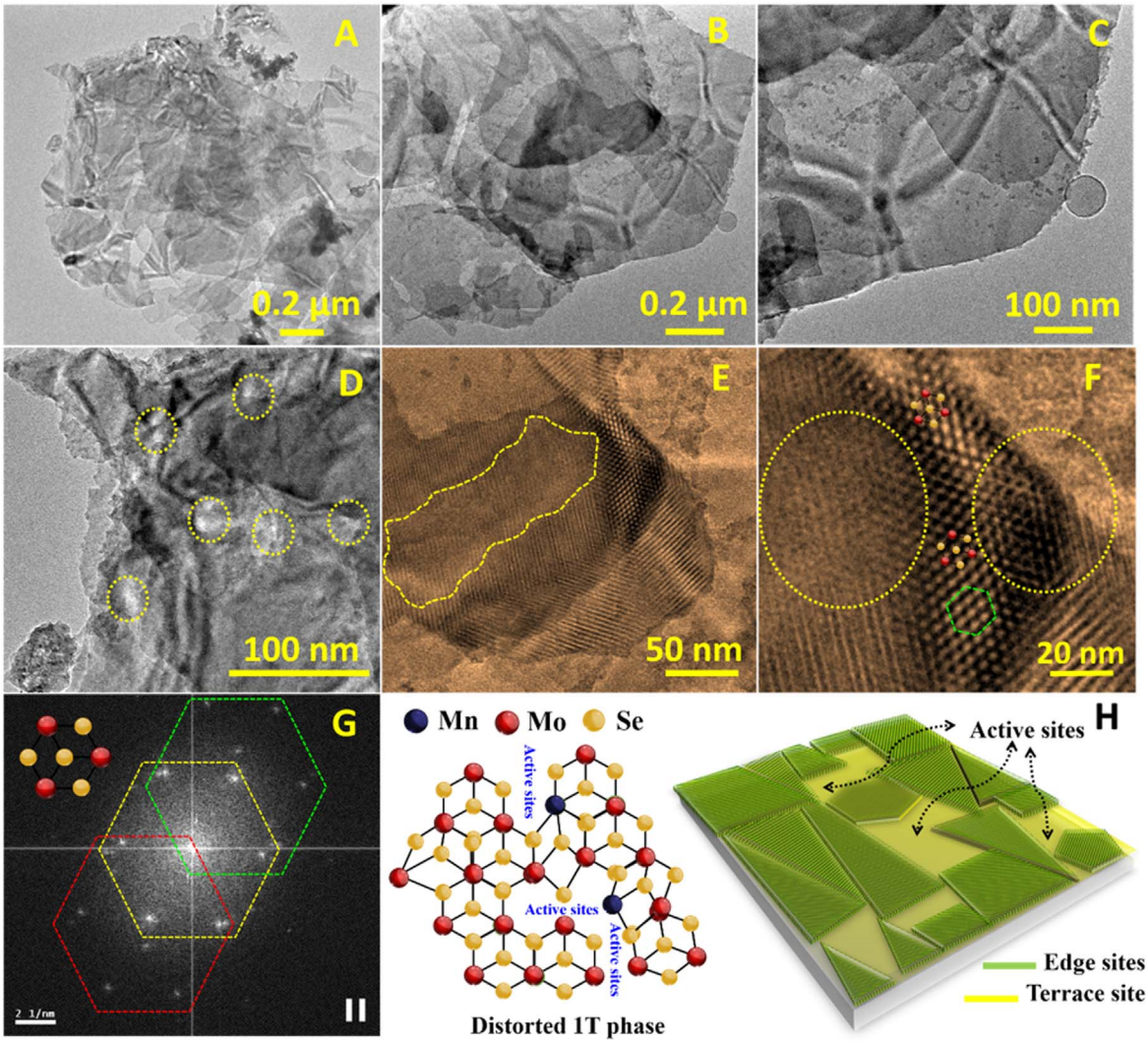

Figure 3. HRTEM images of 1T and distorted phase of Mn doped $MoSe_2$, reproduced from Ramaraj et al.[86] Copyright 2019 American Chemical Society.

have a band alignment in which the conduction band minimum and valence band maximum are located in different monolayers. This gives rise to the formation of interlayer excitons and facilitates interlayer charge transfer, providing a new platform to engineer more efficient electrocatalysts.

Synthesis and formation of TMDs and 2D TMD layered sheets.—Another attractive aspect of TMDs is their facile synthesis. However, it should be noted that the Janus TMDs with two different chalcogen surfaces are considerably more challenging to experimentally form and are typically fabricated using modified chemical vapour deposition (CVD) techniques.[91] In general, TMDs are formed using two main approaches and these are summarised in Table I. The hydrothermal synthesis, where H_2O is employed as the solvent system, is relatively simple, where the precursors are combined and then autoclaved at low temperatures. For example, Sakthivel et al.[92] formed Ni-doped $MoSe_2$ nanoplates by dissolving Na_2MoO_4 and $Ni(NO_3)_2$ in water, followed by the dropwise addition of selenium and hydrazine (reducing agent) over a 30 min period. Then, the reaction mixture was transferred to an autoclave and maintained at 180 °C for 12 h, as illustrated in Fig. 4. Indeed, hydrothermal synthesis can be employed to give different morphologies, including nanoflowers,[93] nanoflakes,[94] nanoplates,[95] nanoparticles[96] and quantum dots.[96] Moreover, hydrothermal synthesis is very suited to the formation of dichalcogenide-based composites or hybrids, where the dichalcogenide is combined with other conducting materials, including carbon nanofibers (CNF),[97] metal nanoparticles[98] and graphene.[99] Furthermore, the dichalcogenides can be grown on different support materials, for example on carbon cloth,[100] and are easily doped with metals and non-metals.[101,102] The dichalcogenides can also be synthesised using solvents other than water. Organic solvents can be employed to alter the viscosity, polarity and solubility of the precursor reagents and intermediates. In this solvothermal synthesis, the precursors are mixed in an organic solvent or polar organic/water mixture with appropriate reducing reagents. The mixture can then be sealed in an autoclave and heated, similar to the hydrothermal approach.[103] Alternatively, the entire synthesis can be carried out using the reflux technique at temperatures in the vicinity of 150 to 320 °C under a nitrogen atmosphere.[104]

In addition, there is considerable interest in chemical vapour deposition (CVD) and vapour phase deposition of the TMDs as these methodologies can be employed to obtain high quality, low-defect, ultrathin, epitaxial films of TMDs on a variety of different substrates.[112,113,115,118,119] The CVD-based methods are ideally suited for the formation of 2D vertically aligned TMDs[120] and Janus structures.[121] Typically, sulfurisation or selenisation of the metal or metal oxide is used and this approach can be employed to give large-area 2D TMDs. The relevant metal, for example Mo[117,122] or a metal oxide, such as WO_3.[123] is initially deposited on a substrate and this is followed by subsequent reactions with the chalcogen vapour. With precise control over the thickness of the metal oxides, which can be achieved using atomic layer deposition, very good control over the number of TMD layers can be accomplished.[122] Attention has also

Table I. A summary of the two main synthetic approaches employed to generate MX_2.

Method	Advantages	MX_2/shape/composites	References
Hydrothermal/Solvothermal	Low temperatures, 100 °C–200 °C, short processing times, economic, suitable for large-scale synthesis, and an environmentally acceptable water-based synthesis. A range of different dichalcogenides in different morphology, and crystallinity, can be readily combined with other materials.	MoS_2 nanostructures	105
	Addition of organic solvents can be used to tune the properties of the final product, including shape, size, efficient, fast and simple approach.	VS_2 quantum dots	106
		$MoSe_2$ nanoflowers	93
		SnS_2 nanoflakes	94
		$FeSe_2$ nanoflakes	107
		MoS_2/MoO_3 nanosheets	108
		Gd-$MoSe_2$/CNF	97
		$ReSe_2$ nanoflakes	109
		WS_2 nanoplates	95
		Co/$CoTe_2$ nanoparticles	96
		CoSe/$MoSe_2$	110
		$EuMoSe_2$ nanoflower	111
		$Mo_{1-x}Nb_xSe_2$ nanosheets	104
		Mesoporous $NiCoSe_2$	103
Chemical Vapour Deposition Methods	High quality, defect-free, thin TMDs with very good adherence to a variety of different substrates. Vertically aligned, Janus and TMD heterostructures can be formed.	MoS_2/ReS_2 heterojunctions	112
		$ZrSe_2$ nanosheets on sapphire	113
		Atomically thin MoS_2	114
		Atomically thin WS_2	115
		$MoSe_2$ on molten glass	116
		$WSe_2/MoSe_2$ heterostructures	117

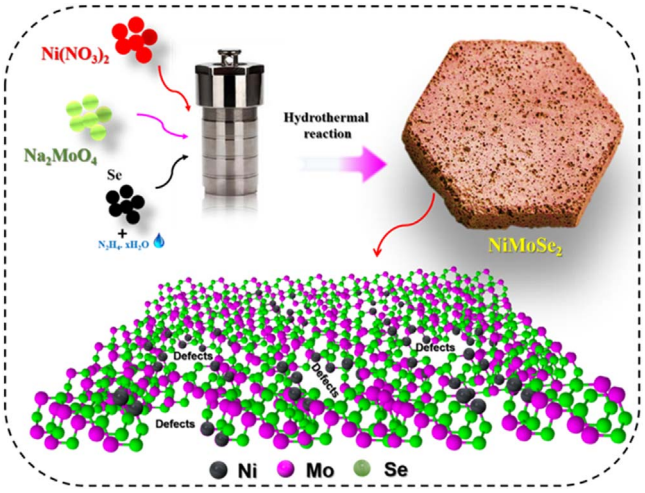

Figure 4. Hydrothermal synthesis of Metal doped $MoSe_2$, reproduced with Sakthivel et al.[92] Copyright 2019 American Chemical Society.

been focused on the thermolysis of suitable Mo and S precursors. For example, ammonium thiomolybdate, which can act as a single precursor, to produce, MoS_2, NH_3 and S vapours, has been employed to give MoS_2.[124] However, polar organic solvents are needed to solubilise these precursors and this can give rise to carbon-containing impurities.

While it is now possible to form two-dimensional (2D) TMDs, including few layered sheets, using chemical vapour deposition, the TMDs are formed as bulk materials in most cases. Therefore, exfoliation of the bulk TMDs is required to give the 2D TMDs. As the dichalcogenide layers are held together by weak van der Waals forces, the bulk TMDs are exfoliated into a few layers. This is normally achieved using methods such as thermal exfoliation, mechanical exfoliation, hydrothermal and liquid-phase exfoliation (LPE).[125] The LPE process is considered to be one of the most efficient exfoliation methods, being cost-effective, scalable and simple, and it has been used to give a variety of low dimensional structures, not only 2D-sheets, but 1D crystals and quantum dots.[126,127] A suitable solvent system is first selected, then the bulk TMDs are normally exfoliated using ultrasound and finally separated using centrifugation. The sonication process uses ultrasound energy to effectively "peel off" layers, from the bulk TMDs. Parameters such as the solvent system, sonication time, and sonication energy are all important. Typically, pyrrolidinone-based organic solvents are used, and while these are very effective, their toxicity and poor environmental acceptability are significant drawbacks. More recently, there has been much focus on the design of water-containing solvent systems and more environmentally acceptable solvent systems such as ethanol[128,129] and isopropanol.[130] Aqueous solutions of macromolecules, including Nafion,[131] alginate[132,133] and chitosan[134] have also been employed in the formation and stabilisation of 2D TMD nanosheets.

While the TMDs are normally first synthesised and exfoliated to give a few sheets of the TMDs, which are then immobilised onto a suitable substrate, it has been shown that electrodeposition can be employed to form TMDs directly at a substrate.[135] For example, Tan and Pumera[136] employed electrosynthesis from an aqueous solution containing ammonium tetrathiotungstate to give highly active WS_{3-x} films for hydrogen evolution. Likewise, Jo et al.[137] employed a nitrate-assisted electrochemical deposition routine to form immobilised NiS and FeSe, that were very effective in the electrolysis of water. Although electrodeposition is a very well established research field, with significant potential for the electrosynthesis of layered TMDs, this approach is still at an early stage of development. Mechanistic insights into the electrodeposition process and more detailed comparisons between the electrosynthesis and chemical

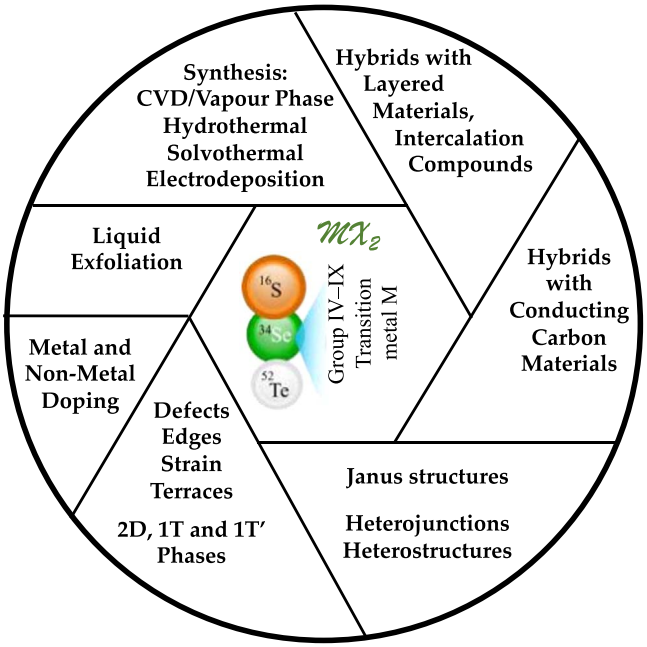

Figure 5. Summary of the versatility of TMDs.

synthesis routines are required to pave the way for the establishment of electrodeposition/electrosynthesis as a suitable methodology for the formation of TMDs directly at various substrates. In conclusion, it is clear that TMDs have great versatility, as summarised in Fig. 5, and are emerging as interesting materials for a range of applications, including electrocatalysts for the splitting of water.

Performance of MoS_2-based electrocatalysts for the HER half-cell.—MoS_2 has been studied extensively as an electrocatalyst for the HER and it is the most widely investigated of all the TMDs for the electrochemical production of hydrogen.[84,138–146] As illustrated earlier, much progress has been made in the synthesis and exfoliation of MoS_2. Some of the more widely used methodologies in the fabrication of MoS_2-modified electrodes involve the dispersion of the MoS_2 sheets in a suitable solvent followed by drop casting[147,148] or spin coating.[149] Alternatively, the MoS_2 can be deposited onto the substrate using chemical vapour deposition,[139] or physical vapour deposition,[150] while it is also possible to combine MoS_2 with non-reactive and inert polymers, such as poly(vinylidene fluoride), and then bake the deposit at about 110 °C.[151]

Typically, the HER activity is measured using polarisation curves and rotating disc voltammetry. The experimental data are fitted to the Tafel equation. This equation, which is the logarithmic approximation of the Butler-Volmer equation, can be described by Eq. 16, where b is the Tafel slope ($b = 2.303RT/\alpha F$) and the intercept can be employed to determine the exchange current density, j_0, ($a = -(2.303RT/\alpha F)\log j_0$). The other parameters in this equation are α, the charge transfer coefficient, F is Faraday's constant, and T represents the thermodynamic temperature. The Tafel slope represents the overpotential required to increase the current density by one order of magnitude and consequently it is a convenient measure of the electrocatalytic activity of the HER electrocatalysts. While the Tafel slope can be employed to formulate mechanistic details, with the theoretical slopes being about 118 mV dec^{-1} for the Volmer reaction, approximately 39 mV dec^{-1} for the Heyrovsky reaction and close to 29.5 mV dec^{-1} for the Tafel reaction, the presence of localised active sites can often make the HER mechanism too complex for this theoretical analysis.[152] Superior electrocatalytic activities are characterised by low Tafel slopes, high exchange current densities and low overpotentials.

Table II. Summary of performance of various MoS_2, doped MoS_2 and MoS_2 heterostructures and composites in the production of $H_2(g)$ in acidic solutions at near room temperatures.

Electro-catalyst	Media	η/mV(10 mA cm^{-2})	Tafel Slope/mV dec^{-1}	Stability	References
1T-MoS_2	H_2SO_4	100	40	—	138
1T-MoS_2	H_2SO_4	187	43	1000 cycles	139
Defective 2H-MoS_2	H_2SO_4	160	46	1000 cycles	147
N-MoS_2	H_2SO_4	168	40.5	5000 cycles	154
Pt-MoS_2	H_2SO_4	100	96	5000 cycles	155
Ru-2H-MoS_2	H_2SO_4	178	77	3000 cycles	156
Fe- MoS_2	H_2SO_4	88	75	24 h	151
Se-O-MoS_2	H_2SO_4	108	47	1000 cycles	149
Ni-MoS_2	H_2SO_4	68	32	10,000 cycles	84
Pt-Pd-MoS_2	H_2SO_4	64	64	—	157
MoS_2/rGO	H_2SO_4	100	41	1000 cycles	158
O,P-MoS_2	H_2SO_4	277 (50 mA cm^{-2})	53	—	140
N-MoS_2	H_2SO_4	168	40.5	5000 cycles	154
N-MoS_2 QDs	H_2SO_4	165	51.2	—	159
MoS_2/CNT/graphene	H_2SO_4	140	100	—	160
MoS_2/Bi_2Te_3/$SrTiO_3$	H_2SO_4	189	58	3000 s	161
MoS_2/Co/NS/CNTs@CoS_2	H_2SO_4	72	59	20 h	162
1T-MoS_2/GO	H_2SO_4	209	45	1000 cycles	163
Co-MoS_2/N,S-rGO	H_2SO_4	178	63	12 h	164
Pt (20 wt% Pt/C)	H_2SO_4	50	33	—	165

$$\eta = a + b \log j \qquad [16]$$

In many of the TMD-based experiments, the HER studies are carried out in nitrogen or argon saturated solutions, using Ag|AgCl or Hg|HgO as the reference electrodes, depending on the pH of the solution. The potential is then converted to the RHE (reversible hydrogen electrode) scale. However, the HER activity is also studied in solutions saturated with hydrogen gas and in these cases, the RHE can be employed as the reference electrode in the cell.[153] This approach has been designed to avoid drifts in the equilibrium potential, which if not stable, can influence the measured kinetics of the HER.[153] Interestingly, in a recent study, it was shown by Xu et al.[153] that the Tafel slopes recorded for Pt(111) in $N_2(g)$ and $H_2(g)$ saturated H_2SO_4 solutions were identical at 30 mV dec^{-1} for overpotentials >50 mV. As the HER currents are high for Pt, the $N_2(g)$ saturated solution becomes saturated with $H_2(g)$ relatively easily. However, deviations were observed at lower overpotentials. Therefore, the presence or absence of hydrogen may influence the kinetics of the TMD-based electrocatalysts at low overpotentials.

The performances of some MoS_2-based electrocatalysts are illustrated in Tables II and III, where the data in Table II illustrate the performance in acidic solution, while the data in Table III, summarise recent studies carried out in alkaline media. The overpotential required to give a current density of 10 mA cm^{-2} is shown in both tables. While this approach is commonly used with Tafel slopes to compare electrocatalysts, exchange current densities are not always provided. Clearly, there is a need to establish a set of activity parameters that can be used more consistently to compare and evaluate the efficiency of electrocatalysts in water splitting. Furthermore, these studies are carried out in simple electrochemical cells and testing in electrolysers under realistic operating conditions may give somewhat different results.

In both media, it is clear that more efficient HER activity can be achieved through doping. Non-metallic dopants, such as N,[154,159,178] O,[179] O combined with P[140] and F and N co-doping[180] have all been employed to improve the HER activity. Indeed Zhang et al.[159] demonstrated that N doping can enhance the conductivity of the MoS_2 basal plane, while Wang et al.[180] have shown that the inert basal plane can also be activated by employing N and F co-doping.

Table III. Summary of performance of various MoS_2, doped MoS_2 and MoS_2 heterostructures and composites in the production of $H_2(g)$ in alkaline solutions at near room temperatures.

MoS_2 composites	Media	η/mV(10 mA cm^{-2})	Tafel Slope/mV dec^{-1}	Stability/Durability	References
MoS_2/$MoSe_2$	KOH	235	96	—	166
MoS_2/WS_2-rGO)	KOH	118	59	20 h	167
MoS_2/CF/graphene/$FeCoNi(OH)_x$	KOH	225 (500 mAcm^{-2})	92	100 h	168
MoS_2/Ni_3S_2/NF	KOH	98	61	48 h	169
MoS_2/Co/NS/CNTs@CoS_2/CC)	KOH	56	43	20 h	162
Fe- MoS_2	KOH	92	49	24 h	151
Ru/Ni-MoS_2	KOH	32	41	20 h	170
Ru-2H-MoS_2	KOH	51	65	3000 cycles	156
$NiCo_2S_4$/1T-MoS_2	KOH	107	66	24 h	171
MoS_2/$Co(PO_3)_2$N-porous carbon	KOH	119	142	20 h	172
MoS_2/CoS_2/PC	KOH	200	93	20 h	173
MOF-derived Co_3O_4/MoS_2	KOH	205	98	12 h	174
Co-O-MoS_2	KOH	113	50	50 h	175
MoS_2/NiCo-LDH	KOH	78	76	48 h	176
Co-MoS_2	KOH	48	52	3000 cycles	36
Pt/C	KOH	20	49	—	177

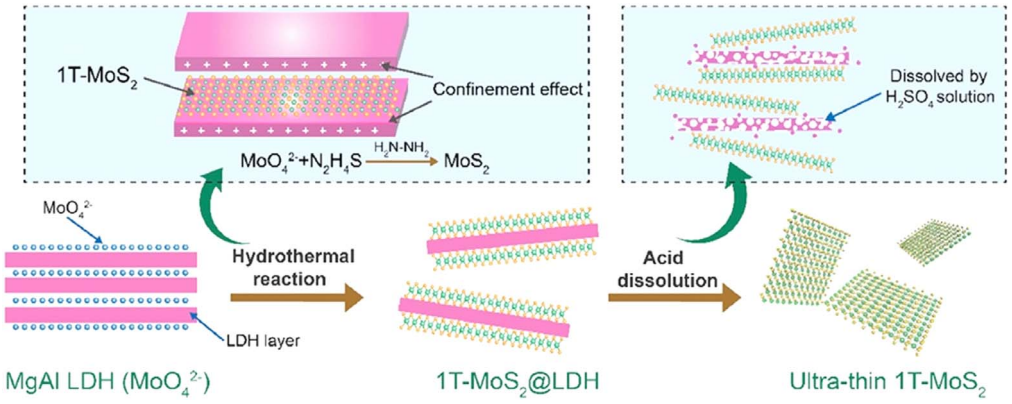

Figure 6. Schematic formation of 1T-MoS_2 by confinement with LDHs. Reproduced with permission from Yang et al.[198] Copyright 2019, Elsevier.

Another approach is to use transition metals as single metal atom dopants or as nanoparticles. Using DFT calculations, Deng et al.[155] concluded that metal atoms in Groups 4 to 8 of the periodic table, including V, Ti, Fe, Mn, Cr, bonded with six S atoms, while metal atoms from Groups 9 to 12, such as Pt, Ag, Pd, Co, and Ni, preferred to bond with only four S atoms. This difference can result in variations in the HER activity as the unsaturated S atoms can facilitate the adsorption of hydrogen atoms. The authors predicted that metal atoms in Groups 4 to 8 would possess low activity, while atomic doping using elements from Groups 9 to 12 could be employed to enhance the HER activity. The authors found that the HER activity of doped MoS_2 varied in the order of Pt > Co > Ni, using experimental measurements, in good agreement with the DFT calculations.[155] Indeed, many of the metal atom dopants in Table II involve elements in Groups 9 to 12, which may be connected to unsaturated S atoms in MoS_2 providing an effective defect engineering strategy.

Another approach involves the coupling of MoS_2 with other conducting materials to form composites or hybrids. In this case, graphene is widely employed as a companion material.[158,163,164,181] For example, it was shown by Li et al.[158] that highly dispersed MoS_2 nanoparticles were formed on graphene sheets, with an abundance of accessible electrocatalytic edge sites. The graphene also provided an interconnected conducting network between the MoS_2 and substrate electrode to give efficient electron transport. In a more recent study, it was found that GO effectively inhibited the transition of MoS_2 from the conducing 1T phase to the semiconducting 2H phase,[163] while Tang et al.[181] employed N-doped rGO combined with MoS_2 nanosheets with enlarged interlayer spacing (9.5 Å). The larger interlayer spacing was achieved by using polyoxometalates, which also gave well dispersed rGO sheets, due to charge repulsion. The authors concluded that the improved HER activity was due to the enlarged interlayer spacing in the MoS_2. Metal doping has also been employed with MoS_2/rGO composites to alter the electronic properties and accordingly improve the electron transfer, with the dopant metals including Zn,[182] Cu,[183–185] Co,[164,186] Ni,[187,188] Pd[189] and Pt.[190] Other carbon-based materials such as carbon nanotubes (CNTs),[191] N-doped CNTs,[192] carbon fibres (CNF) as cloths[193] and foams,[194] and carbon black (CB)[176,195] have been combined with MoS_2 to provide conducting channels and facilitate charge transport along the carbon network. It has also been shown that the density of the highly active terminal disulfide and sulfide groups at the edge of MoS_2 can be tuned by modifying the ratio of the carbon additive (CB) and MoS_2.[195]

Given variations in the experimental measurements and in the synthesis of the MoS_2-based electrodes, including the number of layers, interlayer spacings and intercalated molecules, it is difficult to compare the performance of the MoS_2 composites/hybrids, doped MoS_2 and MoS_2 heterostructures, shown in Tables II and III. However, it is indeed clear that the electrocatalytic activity of 2H-MoS_2 and 1T-MoS_2 can be enhanced through doping, and by forming various hybrid or composite materials. For comparison purposes, the corresponding data are provided for the commercial Pt/C electrocatalysts. Although some of these MoS_2-based electrocatalysts come reasonably close to the performance of the Pt/C, they are still nevertheless not able to compete with the high performing Pt-based electrocatalysts. It is also evident that some of the largest overpotentials are seen in the alkaline solutions. This is consistent with MoS_2 being a relatively good electrocatalyst in acidic media, facilitating the adsorption and recombination of the adsorbed H intermediates. However, it is a poorer electrocatalyst for the water dissociation steps that are associated with the HER process in alkaline solutions.

One avenue that can be employed to improve the sluggish kinetics in alkaline media, involves the use of layered double hydroxides (LDH) and these have been combined with MoS_2. LDHs are layered materials that are very efficient in the adsorption and dissociation of hydroxyl species and it has been shown that MoS_2/NiCo-LDH[176,196] and MoS_2/NiFe-LDH,[197] are efficient electrocatalysts for the HER in alkaline media. As LDHs can be dissolved in acidic media, they can also be employed to give the spatial confinement of MoS_2, resulting in thin layers and rich defects and this has been achieved with MoS_2/MgAl-LDH with intercalated MoO_4^{2-} anions.[198] In the presence of H_2SO_4, the LDHs dissolve to give the 1T-MoS_2, while they are retained in alkaline solutions and are sandwiched between the layered TMDs, as illustrated in Fig. 6.

Performance of the $MoSe_2$-based electrocatalysts for the HER half-cell.—Although the metal disulfides have generated considerable interest in the electrocatalytic generation of $H_2(g)$, transition metal diselenides have more recently been shown to have higher electrochemical activity than their corresponding disulfide counterparts. Furthermore, selenium is more abundant and cost-effective due to its high concentration in minerals and is an essential trace element.[86] Specifically, the metallic property of Se is higher than S, and it has more electroactive unsaturated edge sites, higher metallic binding with transition metals, higher capacitance, a narrower band gap, larger atomic size and polarisability than S.[86] In addition, due to its wide interlayer spacing (0.646 nm), compared with MoS_2 (0.615 nm) and graphene (0.34 nm), the insertion and extraction of electrolyte ions are more efficient.[199] Furthermore, Tsai et al.[200] has shown that $MoSe_2$ has more active edge sites, with both Mo and Se active edges.

In terms of an electrocatalyst for HER, there is very good evidence to show that $MoSe_2$ is a more superior electrocatalyst than MoS_2 for the HER in acidic environments.[79,200–203] For example, Gholamvand et al.[203] compared the HER activity in acidic media of solution-processed films of MoS_2, WS_2, $MoSe_2$, WSe_2, $MoTe_2$ and WTe_2 nanosheets and concluded that the performance varied in the order selenide > sulfide > telluride and $MoSe_2$ exhibited the best performance. Likewise, Tang et al.[201] on comparing MoS_2 with $MoSe_2$ found that the $MoSe_2$ was a better electrocatalyst than MoS_2

Table IV. Summary of performance of various $MoSe_2$-based composites in HER activity, at near room temperature.

$MoSe_2$-based electrocatalysts	Media	η/mV (10 mA cm^{-2})	Tafel Slope/mV dec^{-1}	Stability/Durability cycles/h	References
$MoSe_2$-rGO-CNTs	H_2SO_4	206	46	20 h	215
1T/2H-$MoSe_2$	H_2SO_4	192	48	1000	216
SMoSe nanodots	H_2SO_4	140	40	—	212
N-1T-2H $MoSe_2$/graphene	H_2SO_4	98	49	20000	217
$CoSe_2$/$MoSe_2$/rGO	H_2SO_4	107	56	1000	208
	KOH	182	89		
$FeSe_2$/$MoSe_2$/rGO	H_2SO_4	101	55	1000	218
	KOH	179	80		
1T/2H-$MoSe_2$/Ti_3C_2	KOH	150	90	30 h	210
$MoSe_2$/$CoSe_2$/CFP	KOH	137	55	24 h	205
Perovskite oxide/$MoSe_2$	KOH	128	45	—	219

for the HER and explained this finding in terms of the Gibbs energy change for the adsorption of hydrogen at the electrocatalyst. It is generally accepted that a value close to 0 eV results in a good HER electrocatalyst. Indeed, using DFT calculations, it was shown that $MoSe_2$ has a favourable adsorption energy in acidic media. However, in alkaline solutions, $MoSe_2$ has unfavourable water adsorption and dissociation steps, and for efficient HER activity, additional components are often added. For example, CoSe, which is efficient in the adsorption and dissociation of water, has been combined with $MoSe_2$ to enhance the Volmer step in the alkaline HER.[204,205] Indeed, Shu et al.[206] concluded that with appropriate defects and edges, $MoSe_2$ is able to compete with the Pt-based HER electrocatalysts.

Various methods have been used to enhance the HER performance of $MoSe_2$, and these include the formation of $MoSe_2$ hybrids with conducting materials, such as CNTs,[207] graphene,[208] MXenes,[209,210] and g-C_3N_4 (graphitic carbon nitride).[211] Furthermore, Janus-type TMDs, such as Te-deficient Janus RGO/1T-TeMoSe nanostructures have also shown excellent hydrogen evolution activity,[121] while the promising HER activity of SMoSe nanodots has been attributed to the high-density of active edge sites, basal-plane Se-vacancies coupled with a high-percentage of the 1T phase.[212] There has been a lot of focus on fabricating bimetallic heterostructures for enhancing the HER activity. Heterostructures consisting of $FeSe_2$/$MoSe_2$ were shown to have a higher HER activity than the individual $MoSe_2$ and $FeSe_2$ components.[213] Likewise, the $MoSe_2$/$NiSe_2$ combination was shown to be more superior than its individual components.[214] The very good performance of the $MoSe_2$-based electrocatalysts in the HER is illustrated in Table IV, where it is evident that a number of the electrocatalysts are more efficient than the MoS_2-based system, Tables II–IV. Furthermore, several of the $MoSe_2$ composites/hybrids have low overpotentials accompanied by low Tafel slopes, ranging from 40 to 50 mV dec^{-1} in acidic solutions. Impressive low Tafel slopes with values as low as 45 and 55 mV dec^{-1} have also been observed in alkaline media, Table IV.

TMD-based electrocatalysis for the OER half-cell reaction.— The OER is a sluggish electrochemical reaction in the splitting of water, and accordingly the development of electrocatalysts that do not require high overpotentials is crucial in the design of efficient water electrolysis cells. Furthermore, these electrocatalytic materials need to exhibit good stability when polarised to the relatively high potentials where the OER occurs, >1.23 V vs SHE. While there is clear evidence to show that $MoSe_2$-based electrocatalysts are very efficient in the HER and have a more superior activity than the MoS_2-based systems, the performance of $MoSe_2$ in the OER remains to be critically assessed and fully evaluated. It appears that $MoSe_2$ is a relatively poor electrocatalyst in the OER and therefore it has been combined with copper, nickel or cobalt structures that can facilitate the oxidation of water. For example, the inert basal plane of $MoSe_2$ has been decorated with Cu_2S nanocrystals,[220] Co/Ni nanoparticles to give co-catalysts,[221] and various $CoSe_2$/$MoSe_2$ composites have been employed to facilitate the OER.[222,223]

Furthermore, the partial oxidation of $MoSe_2$ and other TM diselenides can occur when polarised to high potentials. This gives rise to the formation of oxides/hydroxides that can play a significant role in the OER. Indeed, Zhang et al.[222] fabricated ultrathin sheets of $CoSe_2$ with abundant selenium vacancies using a plasma-exfoliation method. The selenium vacancies were used to promote the conversion of $CoSe_2$ to the highly active CoOOH, while the $CoSe_2$ ultrathin sheets served as an efficient transport corridor for the electrolyte. Furthermore, Tang et al.[224] employed $MoSe_2$ nanosheets as a sacrificial template to facilitate the transformation of FeCoMoSe, a trimetallic selenide heterostructure, to an active amorphous FeCo-oxyhydroxide during the OER. Interestingly, the nanosheet morphology was maintained giving rise to an exposed space for the newly formed FeCo-oxyhydroxides. The electrocatalyst showed excellent OER activity with an overpotential of 264 mV at 10 mA cm^{-2} and good stability over 100 h in an alkaline medium. On studying the OER activity of $MoSe_2$/Cu_2S, Hassan et al.[220] observed the formation of an overlayer of copper hydroxide, which can facilitate O–O bond formation and the transformation from M–O to M–OOH, Eqs. 12 and 13. The authors observed the oxidation of Cu (I) to Cu(II), Se(−II) to SeO_x and Mo(IV) to Mo(VI) on the surface of the electrocatalyst, but concluded that the $MoSe_2$/Cu_2S core was preserved during the OER. Likewise, De Silva et al.[225] concluded that the active surface of Ni_3Se_2 and Ni_3Te_2 evolved into a mixed anionic (hydroxo)chalcogenide, with prolonged exposure to KOH, but the dichalcogenide core was retained.

Other reports, where diselenides are employed to facilitate the OER, include the fabrication of $MoSe_2$/$CoSe_2$/CoAl-LDH, which exhibits an overpotential of 320 mV at 10 mA cm^{-2} and a Tafel slope of 71 mV dec^{-1} in KOH.[223] In addition, a $CoSe_2$/$MoSe_2$ composite has been combined with PEDOT, where the conducting polymer was employed to increase the interlayer spacing, minimise aggregation of the diselenide sheets and expose more edge planes. In these cases, there was no discussion on the nature and role of any oxides/hydroxides formed during the OER. While it does appear that diselenide heterostructures have real potential in the OER, more fundamental studies on the nature and role of the oxide/hydroxides or surface hydroxy species that are generated during the OER are needed. This in-situ formation of surface active oxide phases, combined with the layered $MoSe_2$-based structures is an interesting way of enhancing the OER, but it may also reduce the overall stability of the electrocatalysts.

Likewise, the disulfides may exhibit instability in aqueous solutions in the presence of dissolved $O_2(g)$, with the ultimate conversion of MoS_2 into sulfate and molybdate anions.[226] Furthermore, MoS_2 has a relatively poor OER activity, with a weak binding strength between the oxygen-containing intermediates and MoS_2. However, by combining MoS_2 with other materials, such as CoS_2, the energy barriers of the oxygen-containing intermediates are reduced and the composites can become effective in the OER.[173]

Table V. Performance as an alkaline electrolysis cell operating at near room temperature.

Cathode//Anode	Substrate/Electrolyte	Cell Voltage /V	Current density/mA cm^{-2}	Stability >/h	References
MoS_2/CoS_2	Porous C (PC)/KOH	1.59	10	20	173
CoS_2/MoS_2	Carbon cloth (CC)/ KOH	1.59	10	26	245
CoS_2/MoS_2	NF/KOH	1.61	10	10	243
Fe-MoS_2	NF/KOH	1.52	10	25	250
MoS_2/Ni_9S_8	NF/KOH	1.72	50	14	232
MoS_2/Ni_3S_2	NF/KOH	1.54	100	12	251
MoS_2/NiS	CC/KOH	1.54	10	24	252
MoS_2/Ni_3S_2	NF/KOH	1.50	10	48	233
$MoS_2/NiS_2/CoS_2$	Ni foam (NF)/KOH	1.54	10	34	253
$MoS_2/Co_3S_4/Ni_3S_2$	NF/KOH	1.72	50	—	254
MoS_2/NiCoS	NF/KOH	1.50	10	22	255
N-MoS_2/N-Ni_3S_2	NF/KOH	1.79	100	10	244
O-CoS_2/MoS_2	CF/KOH	1.60	10	20	246
$MoWS_2/Ni_3S_2$	NF/KOH	1.62	10	50	256
MoS_2/AB (acetylene black)	NF/KOH	1.51	10	12	257
Gr/MoS_2/$FeCoNiP_x$||Gre/MoS_2/FeCoNi$(OH)_x$	CF/KOH	1.59	100	100	168
CoS-β-$Co(OH)_2/MoS_{2+x}$	NF/KOH	1.58	10	28	258
MoS_2/MXene	NF/KOH	1.64	10	50	259
Perovskite oxide/K-$MoSe_2$	NF/KOH	1.95	100	2500	219
NiSe	CC/KOH	1.52	100	12	135
$NiCo_2Se_4$	CC/KOH	1.58	10	10	260
$NiSe_2/FeSe_2$	Ni-Fe foam/KOH	1.46	10	100	261
Ni_3S_2/1T-MoS_2/Ni_3S_2	Alkaline seawater	1.82	100	100	249
Pt/C||(IrO_2C	KOH	1.65	10	10	262

Consequently, various MoS_2 heterostructures have been formed and considered for the OER, as the heterostructures can provide additional active sites and higher charge transfer. Layered metal hydroxides are especially promising materials for the formation of MoS_2 heterostructures as the LDH has very good performance as an OER electrocatalyst. A number of MoS_2/LDH heterostructures have been formed with impressive OER activity and this has been attributed to electronic interactions between MoS_2 and the LDH.[168] In a recent study, Ji et al.[168] combined MoS_2 nanosheets with graphene and FeCoNi-LDHs to give a very efficient OER electrocatalyst, with a current density of 0.5 A cm^{-2} at an overpotential of 225 mV and a Tafel slope of 29.2 mV dec^{-1} in KOH. Additional LDHs, such as NiFeCr-LDH,[227] CoAl-LDH,[228] CeCoAl-LDH,[229] NiAl-LDH[230] and NiFe-LDH[197] have also been used to form MoS_2/LDH heterostructures for OER, while MoS_2 heterostructures have been formed using cobalt phosphides, which are known as good OER electrocatalysts.[231]

Nickel sulfides are also highly active for OER, and it is no surprise that they have been combined with MoS_2 to give heterostructures, such as MoS_2/Ni_9S_8,[232] MoS_2/Ni_3S_2,[233] $MoS_2/Fe_5Ni_4S_8$,[234] MoS_2/NiS_2 combined with N-doped graphene foams,[235] Ni_3S_2/MoS_2[236] and $MoSe_2/Ni_3S$/FeOOH.[237] Indeed, $MoS_2/Co_9S_8/Ni_3S_2$/Ni has been employed to promote the OER across a wide pH range with overpotentials of 166, 228, and 405 mV in alkaline, acidic, and neutral solutions.[238] The doping of MoS_2 by noble metals and non-metals provides another convenient way to activate the basal plane and Ru-doped CuO/MoS_2,[239] Co-doped MoS_2,[240] and Fe-doped $MoSe_2$[241] have all been employed as an electrocatalyst for OER. While it is clear that various MoS_2-based materials have been fabricated and used successfully as OER electrocatalysts, very little attention has been devoted to the possible dissolution and modification of the $MoSe_2$ during the OER.

TMD-based electrocatalysts in electrolysis cells.—Currently, two commercial electrolyser technologies exist, the well-known proton exchange membrane (PEM), and the alkaline water electrolysers. The PEM cells are efficient, but the highly acidic environment requires corrosion resistant materials such as Pt and Ir electrocatalysts. The TMDs are not sufficiently stable in this acidic environment and are more suited to the alkaline electrolysers and to the more recently proposed anion-exchange membrane water electrolysers. These latter electrolysis cells are attracting significant attention, as they facilitate the use of dilute KOH solutions, or even pure water.[242] The TMD-based electrocatalysts may be effective in the development of these electrolysers as they are likely to be stable in these less aggressive electrolytes.[242]

To ensure good adhesion between the TMDs and the conducting substrate, especially during the evolution of gases, Ni foam (NF),[243,244] carbon cloth (CC),[245] carbon fibre (CF)[246] and porous carbon substrates[173] are normally employed as the substrate supports. It has also been shown that a sulfur-doped carbon (SDC) substrate can facilitate the HER when employed as a support for $CoMoS_4$,[247] indicating the important role of the substrate material. This enhanced activity was attributed to the formation of a new Co_9S_8 phase. Additionally, the porous substrates with large surface areas can serve to facilitate the release of hydrogen and/or oxygen bubbles. As illustrated in Table V, many of the cell potentials recorded in KOH compare very favourably with the traditional noble metal systems, such as RuO_2||Pt/C, which exhibit a cell potential of 1.58 V. However, the challenge with the TMD composites or hybrids as anodes and cathodes in alkaline electrolysis cells is the chemical and structural changes that can occur at the high cell potentials. For example, it has been shown by Hu et al.[248] that on employing 1T-MoS_2/PMoS_2/CoP in an alkaline electrolysis cell that the CoP almost disappeared from the surface, as a result of its partial oxidation to Co oxides/oxyhydroxides (CoOx). While Co-based oxides can be very beneficial as electrocatalysts, these changes to the surface chemical composition can impact the longer term stability of the electrolysis cell. Interestingly, as highlighted in Table V a sandwiched multi-layered Ni_3S_2/1T-MoS_2/Ni_3S_2 composite with good corrosion resistance in chloride-containing electrolytes was successfully employed in salty water splitting.[249] The authors concluded that the central MoS_2 layer gives rise to an electron-deficient Ni_2S_2 layer with superior OER activity, while the Ni_3S_2 layers provided good corrosion protection.

There has been relatively few studies devoted to the application and design of TMD-modified electrodes for the PEM electrolysers, where the electrolyte is a solid polymer electrolyte and the cell operates under acidic conditions. However, in a recent study, Mo et al.[263] incorporated transition metal doped MoS_2 into an industrial-type PEM. The two electrodes were separated by a Nafion 115 membrane. The transition metal atom-doped MoS_2 was processed as an ink and then deposited using spray casting onto one side of the membrane. An IrO_2 OER catalyst and Nafion ionomer solution was sprayed onto the other side of the Nafion membrane and the cell was operated at 80 °C. The authors found that the Co-doped MoS_2 yielded the highest current density, comparing well with the commercial Pt/C electrocatalyst. This was attributed to the fully acidified Nation membrane, which gives rise to a very acidic environment, enabling the efficient adsorption of hydrogen atoms at the MoS_2-based cathode. Similarly, Karikalan et al.[247] formed a single-cell PEM electrolyser using $CoMoS_4$/SDC as the cathode electrocatalyst, IrO_2 as the anode electrocatalyst, and Nafion 117 as the membrane. The electrocatalyst inks were prepared and then brush coated onto the Nafion, followed by hot pressing to give strong adhesion between the electrocatalysts and the membrane. The cell was operated at 27 °C. The PEM cell exhibited impressive stability with no evidence of any deterioration over a 100 h period at 110 mA cm^{-2}. When the $CoMoS_4$ and $CoMoS_4$/SDC membranes were compared, it was found that the simple $CoMoS_4$ showed poor stability and this was attributed to the presence of the SDC, which facilitated the formation of the Co_9S_8 phase in $CoMoS_4$/SDC.

Performance of 2D TMDs in photoelectrochemical water splitting.—Photoelectrochemical (PEC) water splitting integrates water electrolysis with solar energy harvesting and is becoming a promising technology to convert intermittent solar energy into hydrogen. Consequently, electrocatalysts that can not only minimise the overpotential for the HER, but that can facilitate the absorption of light energy, are essential. Furthermore, in order to realise cost-effective and efficient PEC devices, stable and highly active HER photocathodes must be integrated with a semiconductor photo-absorber and relevant cocatalysts. The Si semiconductor, with a band gap of 1.18 eV and with a CB suitable for the HER, has been employed as both the photoanode and photocathode in PEC cells. However its durability, due to surface photo-corrosion and energy conversion efficiency, is still not sufficient for widespread applications. Furthermore, the corrosion of many of the existing semiconductors when exposed to water remains an issue, and as a result different semiconducting oxides have been explored and employed,[264,265] aimed at enhancing the stability of the semiconductors.

Clearly, more efficient new materials or co-catalysts that can be combined with the existing semiconductors to enhance durability and performance are required. Among the various new cost-effective and high surface area semiconductors being considered as photo-electrodes in PEC devices, 2D TMDs are attracting considerable attention, as they exhibit tunable bandgap energies with the potential to absorb photons in the visible, ultraviolet and infrared regions of the electromagnetic spectrum. In this case, it is the 2D, 2H crystal phase (semiconductor) that absorbs light to generate the e^-/h^+ pair. However, the 2D, 1T metallic phase can serve as an electron acceptor and supress the charge recombination process. Accordingly, both the 2H and 1T phases have applications in PEC cells. Furthermore, 2D TMDs have the potential to act as the semiconductor photo-absorber, photocathode where the hydrogen gas is generated, as a co-catalyst or as a semiconductor heterojunction. The co-catalysts serve to capture the excited electrons in the CB and consequently minimise charge recombination reactions. Likewise, hybrid materials consisting of at least two different semiconductors that lead to the formation of a p–n junction, with an alternate layer of a p-type and n-type semiconductor, can reduce charge recombination. This occurs as the electrons accumulate in the n-type region and the holes reside in the p-type region. Consequently, the photoelectrochemical activity is increased as charge recombination is suppressed.[266]

Some 2D TMDs have been employed as a photoelectrode without the addition of another semiconductor or co-catalyst. For example, Liu et al.[120] used 2D vertically aligned SnS_2 nanosheets, Fig. 7a, as photoanodes for PEC water splitting with a high photocurrent density of 1.92 mA cm^{-2} (100 mA cm^{-2} solar energy). However, in most cases, other materials are combined with the TMDs to enhance the production of $H_2(g)$. Indeed, 2D TMDs have been combined with various semiconducting materials and especially with Si to form a range of hybrids. For example, Si nanowire photo-cathode arrays sheathed in TMD layers were formed and it was found that Si/MoS_2, Si/$MoSe_2$, Si/WS_2, and Si/WSe_2 photocathodes all exhibited excellent PEC performance, with photocurrents of 20–30 mA cm^{-2} (at 0 V vs RHE) in 0.5 M H_2SO_4 with negligible degradation of the HER for 3 h under solar irradiation (100 mW cm^{-2}).[267] In another study, vertically aligned MoS_2 nanoflakes formed at SiO_2/Si were used as a photoelectrode with a current density of 0.51 mA cm^{-2} (in 0.5 M H_2SO_4 at −0.8 V (Ag|AgCl), with a 75 W xenon lamp).[268] Likewise, chemically exfoliated 1T-MoS_2 was combined with planar p-Si to give photocathodes for PEC hydrogen generation, Fig. 7b, with a high current density of 17.6 mA cm^{-2} and very good stability.[269]

The modification of TiO_2 with MoS_2 can also significantly enhance the photocatalytic performance and production of hydrogen.[145,270,271] This improved performance is attributed to the transfer of electrons from the CB of TiO_2 to the MoS_2 nanosheets, assisted by the good contact between the 1T-MoS_2 metallic phase and TiO_2.[145] However, in other studies, it has been suggested that the MoS_2/TiO_2 is a heterojunction semiconductor, where the high photocatalytic activity, arises from the transfer of the photo-generated electrons from MoS_2 to TiO_2.[272] This difference in the mechanism of the enhanced PEC activity appears to be connected with the ratio of the 1T-MoS_2 and 2H-MoS_2 phases. Other semiconductors have been integrated with TMDs and these include a MoS_2/g-C_3N_4 heterostructure, which was fabricated using CVD and pulsed laser deposition. It was found that the hybrid had low e^-/h^+ recombination rates, reaching values of 252 μmol h^{-1} for $H_2(g)$ generation rates.[273] Other examples include $Fe_2O_3/BiVO_4/MoS_2$ with a $H_2(g)$ production rate of 46.5 μmol cm^{-2} over 2 h,[274] $MoS_2/ZnIn_2S_4$ giving a maximum rate of 201 μmol h^{-1} for $H_2(g)$,[275] and MoS_2/ZnS with a maximum rate of 606 μmol h^{-1} g^{-1} of $H_2(g)$.[276]

The 2D TMDs are also finding numerous applications as co-catalysts in PEC devices, replacing noble metal photocatalysts. For example, Tiwari et al.[277] employed MoS_2/rGO as a co-catalyst with Cu_2O. This ternary hybrid, Cu_2O/MoS_2/rGO, exhibited a photoelectrochemical current density of 8.46 mA cm^{-2} which was 26 times higher than that observed with Cu_2O. This was attributed to suppression of the charge recombination reaction and inhibition of the photo-corrosion of Cu_2O, giving higher photocurrents and greater stability.

One of the more significant characteristics of 2D TMDs is their ability to stabilise the semiconductor photocatalyst/absorber, by preventing (or partially preventing) the photogenerated holes from attacking or corroding the semiconductor. Photocorrosion of semiconductors is normally associated with the accumulation of photo-induced holes on the outer surface, which cause irreversible oxidation of the semiconductor. This is particularly important as a number of very well-known photocatalysts, including Si, can suffer from severe photocorrosion. The enhanced photostability afforded by 2D TMDs has been observed with Cu_2O,[277] CdS[278,279] and Si semiconductors,[280,281] Furthermore, MoS_2 has been employed as a protective layer for the stabilisation of various Group III–V absorbers, such as GaInAsP/GaAs. In this case, it was found that the thin film MoS_2 modified photo-absorber was >5 times more stable and less prone to corrosion than a PtRu modified surface.[282] Interestingly, it has also been shown that when 2H-MoS_2 is combined with MXenes to form a hybrid electrocatalyst for HER,

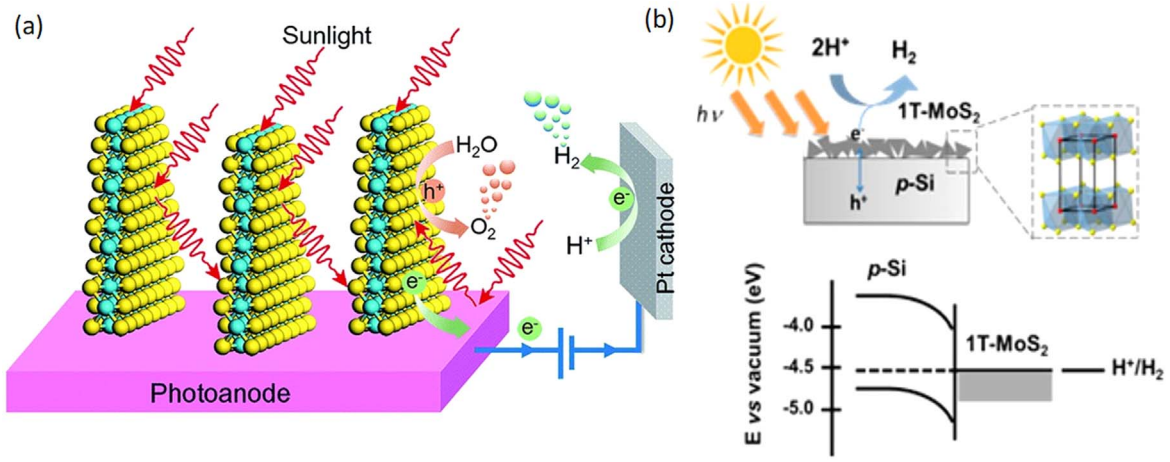

Figure 7. Schematic (a) showing vertically aligned TMDs reproduced with permission from Liu et al.[120] Copyright 2017, Royal Society of Chemistry and (b) the interface heterojunction formed between the Si semiconductor and 1T MoS_2, reproduced with permission from Ding et al.[269] Copyright 2014, American Chemical Society.

its presence suppresses the oxidation of the MXene layers,[283] which are well known to have relatively poor stability in water and are prone to irreversible oxidation.[68]

Another promising recent development is the reported synthesis of Janus TMD monolayers (XMY), where one of the S layers is replaced by Se atoms (SMoSe).[284,285] This has been achieved by exposing a monolayer of MoS_2, formed using CVD, to a H_2(g) plasma to strip the top S layer, Se powder was then introduced to give selenisation and formation of the SMoSe monolayers.[284] These emerging TMDs lack structural symmetry and this gives rise to an intrinsic dipole moment due to the different electronegativities of the two chalcogen atoms. The layer with the lower electronegativity will become positively charged, while the layer with the larger electronegativity will adopt a negative charge. Ji et al.[49] computed dipole moments and electrostatic potentials for a range of Janus TMDs. Dipole moments of 0.19 D and 0.77 D were computed for SMoSe and OMoTe, respectively, with the higher dipole due to the greater difference in electronegativity of the O and Te atoms. Surface potential differences as high as 0.77 eV and 3.26 eV were computed for SMoSe and OMoTe, respectively, and these are sufficient to cause electronic band bending. Indeed, these Janus TMDs can be considered as heterojunction semiconductors, leading to the effective separation of holes and electrons onto the two different surfaces and consequently the photoelectrochemical activity is enhanced. So far the reported studies on the applications of Janus TMDs in PEC devices are computational but these calculations predict that the Janus TMDs have the potential to be ideal photocatalysts in the photoelectrochemical generation of hydrogen.[49,286–289]

Conclusions, Outlook and Future Directions

It is clear that TMDs and especially 2D TMDs are emerging as promising high surface area materials that are effective in the electrocatalytic generation of $H_2(g)$, with potential as OER electrocatalysts and have clear and impressive applications in PEC devices. Although not included in this review, TMDs are also attracting considerable attention in the photocatalytic (PC) splitting of water, where the only inputs are sunlight and water.[290] Very good progress has been made in the synthesis and characterisation of 2D TMDs, metal atom doped 2D TMDs, TMD composites and hybrids, semiconductor heterojunctions and more recently in Janus 2D TMDs. While the bandgap energy can be tailored by tuning the number of 2D layers, defects can be introduced through defect engineering, and TMDs can be combined with a variety of companion materials, the true applications of 2D TMDs are only emerging. Several challenges still remain before 2D TMDs can be employed successfully in HER, OER and PEC applications.

One significant aspect that requires further study is the activation of the basal plane to increase the electronic conductivity of the thermodynamically stable 2H phase. Only the edge sites of the 2H phase are electrocatalytically active. More focus should be placed on increasing the density of edge sites and on activating the inert basal plane. Furthermore, the influence of these activation effects, such as the introduction of chalcogenide vacancies, point defects, and grain boundaries on both the electronic conductivity and overall stability of the semiconducting TMDs is needed. Furthermore, the stability of the 1T-TMDs remains an issue and it is currently difficult to produce and maintain the pure metastable IT or IT' phases. In many cases, the TMDs can exist as a mixture of both the 1T and 2H phases. Although in many publications, where the TMDs are employed as HER electrocatalysts, the durability of the TMDs is assessed over several hours, there is little focus placed on following the changes in phase stability over the experiment. Consequently, surface characterisation techniques, such as high resolution SEM/TEM, XRD and XPS, should not only be carried out on the freshly synthesised TMDs, but also following the HER experiments.

Fortunately, due to the weak van der Waals forces that exist between the TMDs layers, the bulk TMDs can be exfoliated into 2D layers using non-aggressive solution phase processes. However, as with all 2D materials agglomeration of the exfoliated layers can occur and the exfoliation efficiency can vary depending on the composition of the TMDs. This can have a significant effect on the bandgap energy, which depends on the number of TMD layers. More mechanistic insights into the exfoliation mechanisms of the disulfides and diselinides, coupled with the longer term stability of the exfoliated layers, is needed to expand the potential applications of the 2D layered TMDs.

The overall stability of the TMDs, especially when employed as an OER electrocatalyst, remains a concern, with conflicting views on the electroactive sites, with some authors suggesting that the OER occurs at oxide phases that are formed, while others attribute the activity to the TMDs. It is clear that some oxidation of the TMDs occurs when polarised to high potentials and the exact role of these oxide phases is not only relevant to the OER activity, but also important in other potential applications of the TMDs. Likewise, the holes generated on absorption of light energy may lead to a change in the valency of the transition element, with the conversion of Mo (IV) to Mo(V). The role of these potential alterations and the mechanism by which TMDs confer stability and reduce the rate of photocorrosion of a range of semiconductors is not fully understood. One of the more common approaches when employing TMDs in HER, OER and PEC devices is to combine them with other materials to form TMD hybrids and composites. In many cases, especially when combined with semiconductors, interfacial junctions are

formed and the stability of these junctions is critical in terms of the overall stability of the hybrid.

While most studies, including PEC, HER and OER activity, have been carried out in either alkaline (KOH) or acidic (H_2SO_4) electrolytes, relatively few experiments have been carried out in seawater. This is not surprising as this medium has a very high concentration of corrosion promoting chloride anions. However, seawater is an unlimited eco-friendly resource and the development of corrosion resistant or corrosion protected TMD-based electrocatalysts or photoelectrocatalysts would have far reaching applications. Finally, the development of synthetic processes that can be easily scaled-up with more control over morphology and surface defects is needed. Although, CVD-based methods are attractive and can be employed to give vertically aligned TMDs and Janus TMDs that are not achieved using other synthetic methods, they nevertheless lack scalability. The further development of synthetic protocols that can be easily scaled, but can be used to give different morphologies, including both lateral and vertically aligned TMDs will further enhance the applications of TMDs in the energy storage sector.

While a number of challenges remain, TMD nanostructures and especially the 2D TMDs have a promising future in the fabrication of electrocatalysts and photoelectrocatalysts to promote and enhance the HER activity and generate $H_2(g)$. In particular, several 2D TMDs have not yet been considered for the splitting of water, with much of the reported work focussing on MoS_2 and $MoSe_2$. The development of new electrolysers, such as the anion exchange membrane electrolysers, where the electrocatalysts can function in less acidic or basic environments, is also timely as the TMDs are more suited to these less aggressive environments.

Acknowledgments

This publication has emanated from research conducted with the financial support of Science Foundation Ireland under Grant number SFI/20/FFP-P/8793.

ORCID

Carmel B. Breslin https://orcid.org/0000-0002-0586-5375

References

1. O. Hoegh-Guldberg et al., "Coral reefs under rapid climate change and ocean acidification." *Science*, **318**, 1737 (2007).
2. C. Zhao et al., "Temperature increase reduces global yields of major crops in four independent estimates." *Proc. Natl. Acad. Sci. USA*, **114**, 9326 (2017).
3. L. M. Polvani, M. Previdi, M. R. England, G. Chiodo, and K. L. Smith, "Substantial twentieth-century Arctic warming caused by ozone-depleting substances." *Nat. Clim. Chang.*, **10**, 130 (2020).
4. D. J. Kaczan and J. Orgill-Meyer, "The impact of climate change on migration: a synthesis of recent empirical insights." *Clim. Change*, **158**, 281 (2020).
5. M. Yue, H. Lambert, E. Pahon, R. Roche, S. Jemei, and D. Hissel, "Hydrogen energy systems: a critical review of technologies, applications, trends and challenges." *Renew. Sustain. Energy Rev.*, **146**, 111180 (2021).
6. J. Zhu, L. Hu, P. Zhao, L. Y. S. Lee, and K.-Y. Wong, "Recent advances in electrocatalytic hydrogen evolution using nanoparticles." *Chem. Rev.*, **120**, 851 (2020).
7. S. Dresp, F. Dionigi, M. Klingenhof, and P. Strasser, "Direct electrolytic splitting of seawater: opportunities and challenges." *ACS Energy Lett.*, **4**, 933 (2019).
8. J. Turner, G. Sverdrup, M. K. Mann, P.-C. Maness, B. Kroposki, M. Ghirardi, R. J. Evans, and D. Blake, "Renewable hydrogen production." *Int. J. Energy Res.*, **32**, 379 (2008).
9. Q. Cheng, C. Hu, G. Wang, Z. Zou, H. Yang, and L. Dai, "Carbon-defect-driven electroless deposition of Pt atomic clusters for highly efficient hydrogen evolution." *J. Am. Chem. Soc.*, **142**, 5594 (2020).
10. Y. Yao et al., "Engineering the electronic structure of submonolayer Pt on intermetallic Pd_3Pb via charge transfer boosts the hydrogen evolution reaction." *J. Am. Chem. Soc.*, **141**, 19964 (2019).
11. S.-Y. Bae, J. Mahmood, I.-Y. Jeon, and J.-B. Baek, "Recent advances in ruthenium-based electrocatalysts for the hydrogen evolution reaction." *Nanoscale Horizons*, **5**, 43 (2020).
12. S. Cherevko et al., "Oxygen and hydrogen evolution reactions on Ru, RuO_2, Ir, and IrO_2 thin film electrodes in acidic and alkaline electrolytes: a comparative study on activity and stability." *Catal. Today.*, **262**, 170 (2016).
13. A. R. Poerwoprajitno, L. Gloag, S. Cheong, J. J. Gooding, and R. D. Tilley, "Synthesis of low- and high-index faceted metal (Pt, Pd, Ru, Ir, Rh) nanoparticles for improved activity and stability in electrocatalysis." *Nanoscale*, **11**, 18995 (2019).
14. D. Zhao, Z. Zhuang, X. Cao, C. Zhang, Q. Peng, C. Chen, and Y. Li, "Atomic site electrocatalysts for water splitting, oxygen reduction and selective oxidation." *Chem. Soc. Rev.*, **49**, 2215 (2020).
15. C. Zhu, Q. Shi, S. Feng, D. Du, and Y. Lin, "Single-atom catalysts for electrochemical water splitting." *ACS Energy Lett.*, **3**, 1713 (2018).
16. N. Cheng et al., "Platinum single-atom and cluster catalysis of the hydrogen evolution reaction." *Nat. Commun.*, **7**, 13638 (2016).
17. C.-H. Chen, D. Wu, Z. Li, R. Zhang, C.-G. Kuai, X.-R. Zhao, C.-K. Dong, S.-Z. Qiao, H. Liu, and X.-W. Du, "Ruthenium-based single-atom alloy with high electrocatalytic activity for hydrogen evolution, *Adv*." *Energy Mater*, **9**, 1803913 (2019).
18. J. N. Tiwari et al., "High-performance hydrogen evolution by Ru single atoms and nitrided-Ru nanoparticles implanted on N-doped graphitic sheet." *Adv. Energy Mater.*, **9**, 1900931 (2019).
19. L. Liu et al., "Atomic palladium on graphitic carbon nitride as a hydrogen evolution catalyst under visible light irradiation." *Commun. Chem.*, **2**, 18 (2019).
20. X. Gao, Y. Zhou, S. Liu, Z. Cheng, Y. Tan, and Z. Shen, "Single cobalt atom anchored on N-doped graphyne for boosting the overall water splitting." *Appl. Surf. Sci.*, **502**, 144155 (2020).
21. L. Wang et al., "Atomically dispersed Mo supported on metallic Co_9S_8 nanoflakes as an advanced noble-metal-free bifunctional water splitting catalyst working in universal pH conditions." *Adv. Energy Mater.*, **10**, 1903137 (2020).
22. L. Wang, X. Liu, L. Cao, W. Zhang, T. Chen, Y. Lin, H. Wang, Y. Wang, and T. Yao, "Active sites of single-atom iron catalyst for electrochemical hydrogen evolution." *J. Phys. Chem. Lett.*, **11**, 6691 (2020).
23. C. Ling, L. Shi, Y. Ouyang, X. C. Zeng, and J. Wang, "Nanosheet supported single-metal atom bifunctional catalyst for overall water splitting." *Nano Lett.*, **17**, 5133 (2017).
24. J. Yan, L. Kong, Y. Ji, J. White, Y. Li, J. Zhang, P. An, S. Liu, S.-T. Lee, and T. Ma, "Single atom tungsten doped ultrathin α-$Ni(OH)_2$ for enhanced electrocatalytic water oxidation." *Nat. Commun.*, **10**, 2149 (2019).
25. S. Roy, D. Bagchi, L. Dheer, S. C. Sarma, V. Rajaji, C. Narayana, U. V. Waghmare, and S. C. Peter, "Mechanistic insights into the promotional effect of Ni substitution in non-noble metal carbides for highly enhanced water splitting." *Appl. Catal. B Environ.*, **298**, 120560 (2021).
26. W.-F. Chen, J. T. Muckerman, and E. Fujita, "Recent developments in transition metal carbides and nitrides as hydrogen evolution electrocatalysts." *Chem. Commun.*, **49**, 8896 (2013).
27. L. Yu et al., "Non-noble metal-nitride based electrocatalysts for high-performance alkaline seawater electrolysis." *Nat. Commun.*, **10**, 5106 (2019).
28. H. Li, P. Wen, Q. Li, C. Dun, J. Xing, C. Lu, S. Adhikari, L. Jiang, D. L. Carroll, and S. M. Geyer, "Earth-abundant iron diboride (FeB_2) nanoparticles as highly active bifunctional electrocatalysts for overall water splitting." *Adv. Energy Mater.*, **7**, 1700513 (2017).
29. H. Park, A. Encinas, J. P. Scheifers, Y. Zhang, and B. P. T. Fokwa, "Boron-dependency of molybdenum boride electrocatalysts for the hydrogen evolution reaction." *Angew. Chemie - Int. Ed.*, **56**, 5575 (2017).
30. J. Sun, M. Ren, L. Yu, Z. Yang, L. Xie, F. Tian, Y. Yu, Z. Ren, S. Chen, and H. Zhou, "Highly efficient hydrogen evolution from a mesoporous hybrid of nickel phosphide nanoparticles anchored on cobalt phosphosulfide/phosphide nanosheet arrays." *Small*, **15**, 1804272 (2019).
31. Z. Qiu, C.-W. Tai, G. A. Niklasson, and T. Edvinsson, "Direct observation of active catalyst surface phases and the effect of dynamic self-optimization in NiFe-layered double hydroxides for alkaline water splitting." *Energy Environ. Sci.*, **12**, 572 (2019).
32. H. Yang, Z. Chen, P. Guo, B. Fei, and R. Wu, "B-doping-induced amorphization of LDH for large-current-density hydrogen evolution reaction." *Appl. Catal. B Environ.*, **261**, 118240 (2020).
33. Q. Lu, Y. Yu, Q. Ma, B. Chen, and H. Zhang, "2D Transition-metal-dichalcogenide-nanosheet-based composites for photocatalytic and electrocatalytic hydrogen evolution reactions." *Adv. Mater.*, **28**, 1917 (2016).
34. F. Wang, T. A. Shifa, X. Zhan, Y. Huang, K. Liu, Z. Cheng, C. Jiang, and J. He, "Recent advances in transition-metal dichalcogenide based nanomaterials for water splitting." *Nanoscale*, **7**, 19764 (2015).
35. H. Zhou et al., "Efficient hydrogen evolution by ternary molybdenum sulfoselenide particles on self-standing porous nickel diselenide foam." *Nat. Commun.*, **7**, 12765 (2016).
36. Q. Xiong, Y. Wang, P.-F. Liu, L.-R. Zheng, G. Wang, H.-G. Yang, P.-K. Wong, H. Zhang, and H. Zhao, "Cobalt covalent doping in MoS_2 to induce bifunctionality of overall water splitting." *Adv. Mater.*, **30**, 1801450 (2018).
37. X. Wang, A. Vasileff, Y. Jiao, Y. Zheng, and S.-Z. Qiao, "Electronic and structural engineering of carbon-based metal-free electrocatalysts for water splitting." *Adv. Mater.*, **31**, 1803625 (2019).
38. X.-Y. Zhang, H.-P. Li, X.-L. Cui, and Y. Lin, "Graphene/TiO_2 nanocomposites: synthesis, characterization and application in hydrogen evolution from water photocatalytic splitting." *J. Mater. Chem.*, **20**, 2801 (2010).
39. Y. Jiao, Y. Zheng, K. Davey, and S.-Z. Qiao, "Activity origin and catalyst design principles for electrocatalytic hydrogen evolution on heteroatom-doped graphene." *Nat. Energy*, **1**, 16130 (2016).
40. X. Lu, W.-L. Yim, B. H. R. Suryanto, and C. Zhao, "Electrocatalytic oxygen evolution reaction at surface-oxidized multiwalled carbon nanotubes." *J. Am. Chem. Soc.*, **137**, 2901 (2015).
41. T.-Y. Chen, Y.-H. Chang, C.-L. Hsu, K.-H. Wei, C.-Y. Chiang, and L.-J. Li, "Comparative study on MoS_2 and WS_2 for electrocatalytic water splitting." *Int. J. Hydrogen Energy*, **38**, 12302 (2013).

42. C. K. Sumesh and S. C. Peter, "Two-dimensional semiconductor transition metal based chalcogenide based heterostructures for water splitting applications." *Dalt. Trans.*, **48**, 12772 (2019).
43. Y. Sun, K. Xu, Z. Wei, H. Li, T. Zhang, X. Li, W. Cai, J. Ma, H. J. Fan, and Y. Li, "Strong electronic interaction in dual-cation-incorporated $NiSe_2$ nanosheets with lattice distortion for highly efficient overall water splitting." *Adv. Mater.*, **30**, 1802121 (2018).
44. V. D. Nithya, "Recent advances in $CoSe_2$ electrocatalysts for hydrogen evolution reaction." *Int. J. Hydrogen Energy*, **46**, 36080 (2021).
45. J. Li, X. Wang, G. Zhao, C. Chen, Z. Chai, A. Alsaedi, T. Hayat, and X. Wang, "Metal-organic framework-based materials: superior adsorbents for the capture of toxic and radioactive metal ions." *Chem. Soc. Rev.*, **47**, 2322 (2018).
46. T. Zhu, J. Ding, Q. Shao, Y. Qian, and X. Huang, "P,Se-Codoped MoS_2 nanosheets as accelerated electrocatalysts for hydrogen evolution." *ChemCatChem*, **11**, 689 (2019).
47. J. Wu et al., "Exfoliated 2D transition metal disulfides for enhanced electrocatalysis of oxygen evolution reaction in acidic medium." *Adv. Mater. Interfaces*, **3**, 1500669 (2016).
48. U. Gupta and C. N. R. Rao, "Hydrogen generation by water splitting using MoS_2 and other transition metal dichalcogenides." *Nano Energy*, **41**, 49 (2017).
49. Y. Ji, M. Yang, H. Lin, T. Hou, L. Wang, Y. Li, and S.-T. Lee, "Janus structures of transition metal dichalcogenides as the heterojunction photocatalysts for water splitting." *J. Phys. Chem. C*, **122**, 3123 (2018).
50. S. Hong, D. P. Kumar, E. H. Kim, H. Park, M. Gopannagari, D. A. Reddy, and T. K. Kim, "Earth abundant transition metal-doped few-layered MoS_2 nanosheets on CdS nanorods for ultra-efficient photocatalytic hydrogen production." *J. Mater. Chem. A*, **5**, 20851 (2017).
51. M. Chhowalla, H. S. Shin, G. Eda, L.-J. Li, K. P. Loh, and H. Zhang, "The chemistry of two-dimensional layered transition metal dichalcogenide nanosheets." *Nat. Chem.*, **5**, 263 (2013).
52. C. Tan and H. Zhang, "Two-dimensional transition metal dichalcogenide nanosheet-based composites." *Chem. Soc. Rev.*, **44**, 2713 (2015).
53. M. Faraji, M. Yousefi, S. Yousefzadeh, M. Zirak, N. Naseri, T. H. Jeon, W. Choi, and A. Z. Moshfegh, "Two-dimensional materials in semiconductor photoelectrocatalytic systems for water splitting." *Energy Environ. Sci.*, **12**, 59 (2019).
54. X. Cao, C. Tan, X. Zhang, W. Zhao, and H. Zhang, "Solution-processed two-dimensional metal dichalcogenide-based nanomaterials for energy storage and conversion." *Adv. Mater.*, **28**, 6167 (2016).
55. A. Eftekhari, "Molybdenum diselenide ($MoSe_2$) for energy storage, catalysis, and optoelectronics." *Appl. Mater. Today*, **8**, 1 (2017).
56. J. Wei, M. Zhou, A. Long, Y. Xue, H. Liao, C. Wei, and Z. J. Xu, "Heterostructured electrocatalysts for hydrogen evolution reaction under alkaline conditions." *Nano-Micro Lett.*, **10**, 75 (2018).
57. B. Mete, N. S. Peighambardoust, S. Aydin, E. Sadeghi, and U. Aydemir, "Metal-substituted zirconium diboride ($Zr_{1-x}TM_xB_2$; TM = Ni, Co, and Fe) as low-cost and high-performance bifunctional electrocatalyst for water splitting." *Electrochim. Acta*, **389**, 138789 (2021).
58. A. Y. Faid, A. O. Barnett, F. Seland, and S. Sunde, "NiCu mixed metal oxide catalyst for alkaline hydrogen evolution in anion exchange membrane water electrolysis." *Electrochim. Acta*, **371**, 137837 (2021).
59. Y. Kuang et al., "Solar-driven, highly sustained splitting of seawater into hydrogen and oxygen fuels." *Proc. Natl. Acad. Sci. USA.*, **116**, 6624 (2019).
60. L. Wu, L. Yu, F. Zhang, B. McElhenny, D. Luo, A. Karim, S. Chen, and Z. Ren, "Heterogeneous bimetallic phosphide Ni_2P-Fe_2P as an efficient bifunctional catalyst for water/seawater splitting." *Adv. Funct. Mater.*, **31**, 2006484 (2021).
61. G. M. Treacy, A. L. Rudd, and C. B. Breslin, "Electrochemical behaviour of aluminum in the presence of EDTA-containing chloride solutions." *J. Appl. Electrochem.*, **30**, 675 (2000).
62. A. Fujishima and K. Honda, "Electrochemical photolysis of water at a semiconductor electrode." *Nature*, **238**, 37 (1972).
63. H. Zhang, Y. Lu, W. Han, J. Zhu, Y. Zhang, and W. Huang, "Solar energy conversion and utilization: towards the emerging photo-electrochemical devices based on perovskite photovoltaics." *Chem. Eng. J.*, **393**, 124766 (2020).
64. I. Y. Ahmet, Y. Ma, J.-W. Jang, T. Henschel, B. Stannowski, T. Lopes, A. Vilanova, A. Mendes, F. F. Abdi, and R. Van De Krol, "Demonstration of a 50 cm^2 $BiVO_4$ tandem photoelectrochemical-photovoltaic water splitting device." *Sustain. Energy Fuels*, **3**, 2366 (2019).
65. J. Li, Z. Chen, H. Yang, Z. Yi, X. Chen, W. Yao, T. Duan, P. Wu, G. Li, and Y. Yi, "Tunable broadband solar energy absorber based on monolayer transition metal dichalcogenides materials using au nanocubes." *Nanomaterials*, **10**, 257 (2020).
66. J. Wang, H. Shu, T. Zhao, P. Liang, N. Wang, D. Cao, and X. Chen, "Intriguing electronic and optical properties of two-dimensional Janus transition metal dichalcogenides." *Phys. Chem. Chem. Phys.*, **20**, 18571 (2018).
67. Y. Luo, S. Wang, K. Ren, J.-P. Chou, J. Yu, Z. Sun, and M. Sun, "Transition-metal dichalcogenides/$Mg(OH)_2$ van der Waals heterostructures as promising water-splitting photocatalysts: A first-principles study." *Phys. Chem. Chem. Phys.*, **21**, 1791 (2019).
68. T. Yu and C. B. Breslin, "Review—Two-dimensional titanium carbide MXenes and their emerging applications as electrochemical sensors." *J. Electrochem. Soc.*, **167**, 037514 (2020).
69. R. Sukanya, T. N. Barwa, Y. Luo, E. Dempsey, and C. B. Breslin, "Emerging layered materials and their applications in the corrosion protection of metals and alloys." *Sustain.*, **14**, 4079 (2022).
70. S. Manzeli, D. Ovchinnikov, D. Pasquier, O. V. Yazyev, and A. Kis, "2D transition metal dichalcogenides." *Nat. Rev. Mater.*, **2**, 17033 (2017).
71. L. Sun, M. Gao, Z. Jing, Z. Cheng, D. Zheng, H. Xu, Q. Zhou, and J. Lin, "1T-Phase enriched P doped WS_2 nanosphere for highly efficient electrochemical hydrogen evolution reaction." *Chem. Eng. J.*, **429**, 132187 (2022).
72. A. Hamill et al., "Two-fold symmetric superconductivity in few-layer $NbSe_2$." *Nat. Phys.*, **17**, 949 (2021).
73. S. Ramaraj, M. Sakthivel, S.-M. Chen, B.-S. Lou, and K.-C. Ho, "Defect and additional active sites on the basal plane of manganese-doped molybdenum diselenide for effective enzyme immobilization: in vitro and in Vivo real-time analyses of hydrogen peroxide sensing." *ACS Appl. Mater. Interfaces*, **11**, 7862 (2019).
74. M. S. Sokolikova, P. C. Sherrell, P. Palczynski, V. L. Bemmer, and C. Mattevi, "Direct solution-phase synthesis of 1T' WSe_2 nanosheets." *Nat. Commun.*, **10**, 712 (2019).
75. Q. Tang and D.-E. Jiang, "Mechanism of hydrogen evolution reaction on 1T-MoS_2 from first principles." *ACS Catal.*, **6**, 4953 (2016).
76. Z. Lai et al., "Metastable 1T′-phase group VIB transition metal dichalcogenide crystals." *Nat. Mater.*, **20**, 1113 (2021).
77. R. Kappera et al., "Metallic 1T phase source/drain electrodes for field effect transistors from chemical vapor deposited MoS_2." *APL Mater.*, **2**, 092516 (2014).
78. M. Z. M. Nasir, C. C. Mayorga-Martinez, Z. Sofer, and M. Pumera, "Two-dimensional 1T-phase transition metal dichalcogenides as nanocarriers to enhance and stabilize enzyme activity for electrochemical pesticide detection." *ACS Nano*, **11**, 5774 (2017).
79. A. Ambrosi, Z. Sofer, and M. Pumera, "2H → 1T phase transition and hydrogen evolution activity of MoS_2, $MoSe_2$, WS_2 and WSe_2 strongly depends on the MX_2 composition." *Chem. Commun.*, **51**, 8450 (2015).
80. R. Zhou, H. Wang, J. Chang, C. Yu, H. Dai, Q. Chen, J. Zhou, H. Yu, G. Sun, and W. Huang, "Ammonium intercalation induced expanded 1T-rich molybdenum diselenides for improved lithium ion storage." *ACS Appl. Mater. Interfaces*, **13**, 17459 (2021).
81. Y. Ouyang, C. Ling, Q. Chen, Z. Wang, L. Shi, and J. Wang, "Activating inert basal planes of MoS_2 for hydrogen evolution reaction through the formation of different intrinsic defects." *Chem. Mater.*, **28**, 4390 (2016).
82. S. Ramki, R. Sukanya, S.-M. Chen, M. Sakthivel, and J. Y. Wang, "Simple hydrothermal synthesis of defective $CeMoSe_2$ dendrites as an effective electrocatalyst for the electrochemical sensing of 4-nitrophenol in water samples." *New J. Chem.*, **43**, 17200 (2019).
83. G. Ye, Y. Gong, J. Lin, B. Li, Y. He, S. T. Pantelides, W. Zhou, R. Vajtai, and P. M. Ajayan, "Defects engineered monolayer MoS_2 for improved hydrogen evolution reaction." *Nano Lett.*, **16**, 1097 (2016).
84. A. K. Kunhiraman, M. Bradha, and R. A. Rakkesh, "Nickel-doped two-dimensional molybdenum disulfide for electrochemical hydrogen evolution reaction." *J. Mater. Res.*, **36**, 4141 (2021).
85. W. Huang, D. Zhou, G. Qi, and X. Liu, "Fe-doped MoS_2 nanosheets array for high-current-density seawater electrolysis." *Nanotechnology*, **32**, 415403 (2021).
86. S. Ramaraj, M. Sakthivel, S.-M. Chen, and K.-C. Ho, "Active-site-rich 1T-phase $CoMoSe_2$ integrated graphene oxide nanocomposite as an efficient electrocatalyst for electrochemical sensor and energy storage applications." *Anal. Chem.*, **91**, 8358 (2019).
87. H.-Y. He, Z. He, and Q. Shen, "Novel assembly of Janus RGO/1T-SeMoS nanosheets structures showing high-efficient electrocatalytic activity for hydrogen evolution." *Colloids Interface Sci. Commun.*, **45**, 100509 (2021).
88. S. P. Kaur and T. J. D. Kumar, "Tuning structure, electronic, and catalytic properties of non-metal atom doped Janus transition metal dichalcogenides for hydrogen evolution." *Appl. Surf. Sci.*, **552**, 149146 (2021).
89. M. Idrees, H. U. Din, S. U. Rehman, M. Shafiq, Y. Saeed, H. D. Bui, C. V. Nguyen, and B. Amin, "Electronic properties and enhanced photocatalytic performance of van der Waals heterostructures of ZnO and Janus transition metal dichalcogenides." *Phys. Chem. Chem. Phys.*, **22**, 10351 (2020).
90. D. Vikraman, S. Hussain, S. A. Patil, L. Truong, A. A. Arbab, S. H. Jeong, S.-H. Chun, J. Jung, and H.-S. Kim, "Engineering $MoSe_2$/WS_2 hybrids to replace the scarce platinum electrode for hydrogen evolution reactions and dye-sensitized solar cells." *ACS Appl. Mater. Interfaces*, **13**, 5061 (2021).
91. K. Zhang et al., "Enhancement of van der Waals interlayer coupling through polar Janus MoSSe." *J. Am. Chem. Soc.*, **142**, 17499 (2020).
92. M. Sakthivel, S. Ramaraj, S.-M. Chen, T.-W. Chen, and K.-C. Ho, "Transition-metal-doped molybdenum diselenides with defects and abundant active sites for efficient performances of enzymatic biofuel cell and supercapacitorapplications." *ACS Appl. Mater. Interfaces*, **11**, 18483 (2019).
93. J. Wu, Y. Liu, Y. Yao, Y. Shao, and X. Wu, "Graphene-like 2H/1T-$MoSe_2$ with superior full spectrum absorption: Morphology and phase engineering." *J. Alloys Compd.*, **877**, 160317 (2021).
94. H. Tian, C. Fan, G. Liu, Y. Zhang, M. Wang, and E. Li, "Hydrothermal synthesis and fast photoresponsive characterization of SnS_2 hexagonal nanoflakes." *J. Mater. Sci.*, **54**, 2059 (2019).
95. S. Sengupta and M. Kundu, "Carbon free nanostructured plate like WS_2 with excellent lithium storage properties." *ChemistrySelect*, **5**, 14183 (2020).
96. Y. Qi, J. Wu, J. Xu, H. Gao, Z. Du, B. Liu, L. Liu, and D. Xiong, "One-step fabrication of a self-supported Co@$CoTe_2$ electrocatalyst for efficient and durable oxygen evolution reactions." *Inorg. Chem. Front*, **7**, 2523 (2020).
97. N. Jeromiyas, C.-M. Lin, L. Yu-Chieh, C.-H. Chen, V. Mani, R. Arumugam, and S.-T. Huang, "Gd doped molybdenum selenide/carbon nanofibers: An excellent electrocatalyst for monitoring endogenous H_2S." *Inorg. Chem. Front*, **8**, 2871 (2021).
98. S. Shanmugaratnam, D. Velauthapillai, P. Ravirajan, A. A. Christy, and Y. Shivatharsiny, "CoS_2/TiO_2 nanocomposites for hydrogen production under UV irradiation." *Materials (Basel)*, **12**, 03882 (2019).

99. A. Gowrisankar, A. L. Sherryn, and T. Selvaraju, "In situ integrated 2D reduced graphene oxide nanosheets with MoSSe for hydrogen evolution reaction and supercapacitor application." *Appl. Surf. Sci. Adv.*, **3**, 100054 (2021).
100. J. Zhou, Y. Liu, Z. Zhang, Z. Huang, X. Chen, X. Ren, L. Ren, X. Qi, and J. Zhong, "Hierarchical $NiSe_2$ sheet-like nano-architectures as an efficient and stable bifunctional electrocatalyst for overall water splitting: Phase and morphology engineering." *Electrochim. Acta*, **279**, 95 (2018).
101. L. Ji et al., "One-pot synthesis of porous 1T-phase MoS_2 integrated with single-atom Cu doping for enhancing electrocatalytic hydrogen evolution reaction." *Appl. Catal. B Environ.*, **251**, 87 (2019).
102. M. I. Khan et al., "Effect of Ni doping on the structural, optical and photocatalytic activity of MoS_2, prepared by hydrothermal method." *Mater. Res. Express*, **7**, 015061 (2020).
103. P. Santhoshkumar, N. Shaji, G. S. Sim, M. Nanthagopal, J. W. Park, and C. W. Lee, "Facile and solvothermal synthesis of rationally designed mesoporous $NiCoSe_2$ nanostructure and its improved lithium and sodium storage properties." *Appl. Mater. Today*, **21**, 100807 (2020).
104. I. S. Kwon, I. H. Kwak, J. Y. Kim, T. T. Debela, Y. C. Park, J. Park, and H. S. Kang, "Concurrent vacancy and adatom defects of $Mo_{1-x}Nb_xSe_2$ alloy nanosheets enhance electrochemical performance of hydrogen evolution reaction." *ACS Nano*, **15**, 5467 (2021).
105. N. J. A. Cordeiro, C. Gaspar, M. J. de Oliveira, D. Nunes, P. Barquinha, L. Pereira, E. Fortunato, R. Martins, E. Laureto, and S. A. Lourenço, "Fast and low-cost synthesis of MoS_2 nanostructures on paper substrates for near-infrared photodetectors." *Appl. Sci.*, **11**, 1 (2021).
106. D. Yang et al., "One-step synthesis of high-quality vanadium disulfide quantum dots for long-term lysosome-targetable imaging." *Sensors Actuators B Chem.*, **346**, 130544 (2021).
107. Y. Chen, J. Zhang, H. Liu, and Z. Wang, "Controlled synthesis of $FeSe_2$ nanoflakes toward advanced sodium storage behavior integrated with ether-based electrolyte." *Nano*, **13**, 1850141 (2018).
108. S. Duraisamy, A. Ganguly, P. K. Sharma, J. Benson, J. Davis, and P. Papakonstantinou, "One-step hydrothermalsynthesis of phase-engineered MoS_2/MoO_3 electrocatalysts for hydrogen evolution reaction." *ACS Appl. Nano Mater.*, **4**, 2642 (2021).
109. Y. Yan, S. Xu, H. Li, N. C. S. Selvam, J. Y. Lee, H. Lee, and P. J. Yoo, "Perpendicularly anchored $ReSe_2$ nanoflakes on reduced graphene oxide support for highly efficient hydrogen evolution reactions." *Chem. Eng. J.*, **405**, 126728 (2021).
110. W. Song, K. Wang, G. Jin, Z. Wang, C. Li, X. Yang, and C. Chen, "Two-step hydrothermal synthesis of CoSe/$MoSe_2$ as hydrogen evolution electrocatalysts in acid and alkaline electrolytes." *Chem. Electro. Chem*, **6**, 4842 (2019).
111. M. Sakthivel, R. Sukanya, and S.-M. Chen, "Fabrication of europium doped molybdenum diselenide nanoflower based electrochemical sensor for sensitive detection of diphenylamine in apple juice." *Sensors Actuators, B Chem.*, **273**, 616 (2018).
112. J. Yao, H. Liu, Q. He, K. Chen, Y. Wu, X. Li, C. Zhang, Z. Wu, and J. Kang, "Controllable growth of 2H-1T′ MoS_2/ReS_2 heterostructures via chemical vapor deposition." *Appl. Surf. Sci.*, **572**, 151438 (2022).
113. Y. Tian, M. Zheng, Y. Cheng, Z. Yin, J. Jiang, G. Wang, J. Chen, X. Li, J. Qi, and X. Zhang, "Epitaxial growth of $ZrSe_2$ nanosheets on sapphire: via chemical vapor deposition for optoelectronic application." *J. Mater. Chem. C*, **9**, 13954 (2021).
114. A. S. Sindhu, N. B. Shinde, S. Harish, M. Navaneethan, and S. K. Eswaran, "Recoverable and reusable visible-light photocatalytic performance of CVD grown atomically thin MoS_2 films." *Chemosphere*, **287**, 132347 (2022).
115. N. Babu Shinde, B. Deul Ryu, C.-H. Hong, B. Francis, S. Chandramohan, S. Kumar Eswaran, and G. Behavior, "Nucleation control and excellent optical properties of atomically thin WS_2 thin films processed via gas-phase chemical vapor deposition." *Appl. Surf. Sci.*, **568**, 150908 (2021).
116. J. Chen et al., "Chemical vapor deposition of large-size monolayer $MoSe_2$ crystals on molten glass." *J. Am. Chem. Soc.*, **139**, 1073 (2017).
117. Y. Gong et al., "Two-step growth of two-dimensional $WSe_2/MoSe_2$ heterostructures." *Nano Lett.*, **15**, 6135 (2015).
118. J. Li, S. Kolekar, Y. Xin, P. M. Coelho, K. Lasek, F. A. Nugera, H. R. Gutiérrez, and M. Batzill, "Thermal phase control of two-dimensional Pt-chalcogenide (Se and Te) ultrathin epitaxial films and nanocrystals." *Chem. Mater.*, **33**, 8018 (2021).
119. X. Chen, B. Huet, T. H. Choudhury, J. M. Redwing, T.-M. Lu, and G.-C. Wang, "Orientation domain dispersions in wafer scale epitaxial monolayer WSe_2 on sapphire." *Appl. Surf. Sci.*, **567**, 150798 (2021).
120. G. Liu, Z. Li, T. Hasan, X. Chen, W. Zheng, W. Feng, D. Jia, Y. Zhou, and P. Hu, "Vertically aligned two-dimensional SnS_2 nanosheets with a strong photon capturing capability for efficient photoelectrochemical water splitting." *J. Mater. Chem. A*, **5**, 1989 (2017).
121. P. Chen, "Assembly of Janus RGO/1T′-TeMoSe nanostructures possessing enhanced electrocatalytic activity for hydrogen evolution." *Mater. Sci. Semicond. Process.*, **138**, 106253 (2022).
122. Y. Lee, J. Lee, H. Bark, I.-K. Oh, G. H. Ryu, Z. Lee, H. Kim, J. H. Cho, J.-H. Ahn, and C. Lee, "Synthesis of wafer-scale uniform molybdenum disulfide films with control over the layer number using a gas phase sulfur precursor." *Nanoscale*, **6**, 2821 (2014).
123. A. L. Elías et al., "Controlled synthesis and transfer of large-area WS_2 sheets: from single layer to few layers." *ACS Nano*, **7**, 5235 (2013).
124. Y. Shi et al., "Van der waals epitaxy of MoS_2 layers using graphene as growth templates." *Nano Lett.*, **12**, 2784 (2012).
125. L.-C. Wang, S.-K. Bao, J. Luo, Y.-H. Wang, Y.-C. Nie, and J.-P. Zou, "Efficient exfoliation of bulk MoS_2 to nanosheets by mixed-solvent refluxing method." *Int. J. Hydrogen Energy*, **41**, 10737 (2016).
126. T. Chowdhury, E. C. Sadler, and T. J. Kempa, "Progress and prospects in transition-metal dichalcogenide research beyond 2D." *Chem. Rev.*, **120**, 12563 (2020).
127. M. Aleksandrzak, M. Baca, M. Pacia, K. Wenelska, B. Zielinska, R. J. Kalenczuk, and E. Mijowska, "0D, 1D, 2D molybdenum disulfide functionalized by 2D polymeric carbon nitride for photocatalytic water splitting." *Nanotechnology*, **32**, 355703 (2021).
128. N. S. Taghavi and R. Afzalzadeh, "The effect of sonication parameters on the thickness of the produced MoS_2 nano-flakes." *Arch. Acoust.*, **46**, 31 (2021).
129. Y. Zhao, W. Gao, Y. Yang, H. Zhang, C. Redshaw, X. Feng, J. Li, J. W. Y. Lam, and B. Z. Tang, "Aggregation-induced emission luminogens for direct exfoliation of 2D layered materials in ethanol." *Adv. Mater. Interfaces*, **7**, 2000795 (2020).
130. W. Zhao, T. Jiang, Y. Shan, H. Ding, J. Shi, H. Chu, and A. Lu, "Direct exfoliation of natural SiO_2-containing molybdenite in isopropanol: a cost efficient solution for large-scale production of MoS_2 nanosheetes." *Nanomaterials*, **8**, 843 (2018).
131. N. K. Oh et al., "Nafion-mediated liquid-phase exfoliation of transition metal dichalcogenides and direct application in hydrogen evolution reaction." *Chem. Mater.*, **30**, 4658 (2018).
132. D. Xuan, Y. Zhou, W. Nie, and P. Chen, "Sodium alginate-assisted exfoliation of MoS_2 and its reinforcement in polymer nanocomposites." *Carbohydr. Polym.*, **155**, 40 (2017).
133. C.-Y. Lee, A. Prasannan, V. Lincy, S. Vetri Selvi, S. −M. Chen, and P.-D. Hong, "Highly exfoliated functionalized MoS_2 with sodium alginate-polydopamine conjugates for electrochemical sensing of cardio-selective β-blocker by voltammetric methods." *Microchim. Acta*, **188**, 103 (2021).
134. D. C. da Silva Alves, B. Healy, L. A. A. Pinto, T. R. S. Cadaval, and C. B. Breslin, "Recent developments in chitosan-based adsorbents for the removal of pollutants from aqueous environments." *Molecules*, **26**, 594 (2021).
135. D. Chen, Y. Chen, W. Zhang, and R. Cao, "Nickel selenide from single-molecule electrodeposition for efficient electrocatalytic overall water splitting." *New J. Chem.*, **45**, 351 (2021).
136. S. M. Tan and M. Pumera, "Bottom-up electrosynthesis of highly active tungsten sulfide (WS_{3-x}) films for hydrogen evolution." *ACS Appl. Mater. Interfaces*, **8**, 3948 (2016).
137. S. Jo, K. B. Lee, and J. I. Sohn, "Direct electrosynthesis of selective transition-metal chalcogenides as functional catalysts with a tunable activity for efficient water electrolysis." *ACS Sustain. Chem. Eng.*, **9**, 14911 (2021).
138. D. Voiry, M. Salehi, R. Silva, T. Fujita, M. Chen, T. Asefa, V. B. Shenoy, G. Eda, and M. Chhowalla, "Conducting MoS_2 nanosheets as catalysts for hydrogen evolution reaction." *Nano Lett.*, **13**, 6222 (2013).
139. M. A. Lukowski, A. S. Daniel, F. Meng, A. Forticaux, L. Li, and S. Jin, "Enhanced hydrogen evolution catalysis from chemically exfoliated metallic MoS_2 nanosheets." *J. Am. Chem. Soc.*, **135**, 10274 (2013).
140. J. Liu, Z. Wang, J. Li, L. Cao, Z. Lu, and D. Zhu, "Structure Engineering of MoS_2 via simultaneous oxygen and phosphorus incorporation for improved hydrogen evolution." *Small*, **16**, 1905738 (2020).
141. L. Li et al., "Role of sulfur vacancies and undercoordinated Mo regions in MoS_2 nanosheets toward the evolution of hydrogen." *ACS Nano*, **13**, 6824 (2019).
142. X. Wang et al., "Single-atom vacancy defect to trigger high-efficiency hydrogen evolution of MoS_2." *J. Am. Chem. Soc.*, **142**, 4298 (2020).
143. Y. Huang et al., "Atomically engineering activation sites onto metallic 1T-MoS_2 catalysts for enhanced electrochemical hydrogen evolution." *Nat. Commun.*, **10**, 982 (2019).
144. K. Qi et al., "Single-atom cobalt array bound to distorted 1T MoS_2 with ensemble effect for hydrogen evolution catalysis." *Nat. Commun.*, **10**, 5231 (2019).
145. Y. Liu, Y. Li, F. Peng, Y. Lin, S. Yang, S. Zhang, H. Wang, Y. Cao, and H. Yu, "2H- and 1T- mixed phase few-layer MoS_2 as a superior to Pt co-catalyst coated on TiO_2 nanorod arrays for photocatalytic hydrogen evolution." *Appl. Catal. B Environ.*, **241**, 236 (2019).
146. Q. Xu, Y. Liu, H. Jiang, Y. Hu, H. Liu, and C. Li, "Unsaturated sulfur edge engineering of strongly coupled MoS_2 nanosheet–carbon macroporous hybrid catalyst for enhanced hydrogen generation." *Adv. Energy Mater.*, **9**, 1802553 (2019).
147. Y. Li, K. Yin, L. Wang, X. Lu, Y. Zhang, Y. Liu, D. Yan, Y. Song, and S. Luo, "Engineering MoS_2 nanomesh with holes and lattice defects for highly active hydrogen evolution reaction." *Appl. Catal. B Environ*, **239**, 537 (2018).
148. J. Xie, H. Zhang, S. Li, R. Wang, X. Sun, M. Zhou, J. Zhou, X. W. Lou, and Y. Xie, "Defect-rich MoS_2 ultrathin nanosheets with additional active edge sites for enhanced electrocatalytic hydrogen evolution." *Adv. Mater.*, **25**, 5807 (2013).
149. L. Jiang, Y.-J. Zhang, X.-H. Luo, L. Yu, H.-X. Li, and Y.-J. Li, "Se and O co-insertion induce the transition of MoS_2 from 2H to 1T phase for designing high-active electrocatalyst of hydrogen evolution reaction." *Chem. Eng. J.*, **425**, 130611 (2021).
150. D. Kong, H. Wang, J. J. Cha, M. Pasta, K. J. Koski, J. Yao, and Y. Cui, "Synthesis of MoS_2 and $MoSe_2$ films with vertically aligned layers." *Nano Lett.*, **13**, 1341 (2013).
151. D. Vikraman, S. Hussain, K. Karuppasamy, A. Kathalingam, E.-B. Jo, A. Sanmugam, J. Jung, and H.-S. Kim, "Engineering the active sites tuned MoS_2 nanoarray structures by transition metal doping for hydrogen evolution and supercapacitor applications." *J. Alloys Compd.*, **893**, 162271 (2022).
152. T. Shinagawa, A. T. Garcia-Esparza, and K. Takanabe, "Insight on Tafel slopes from a microkinetic analysis of aqueous electrocatalysis for energy conversion." *Sci Rep.*, **5**, 13801 (2015).
153. M. Le, X. , J. Wei, W. Chen, Z. Wei, Q. X. Li, J. Cai, and Y.-X. Chen, "Effect of hydrogen pressure on the intrinsic kinetics of hydrogen evolution reaction at Pt (111) electrode." *J. Electrochem. Soc.*, **169**, 036505 (2022).

154. R. Li, L. Yang, T. Xiong, Y. Wu, L. Cao, D. Yuan, and W. Zhou, "Nitrogen doped MoS_2 nanosheets synthesized via a low-temperature process as electrocatalysts with enhanced activity for hydrogen evolution reaction." *J. Power Sources*, **356**, 133 (2017).
155. J. Deng, H. Li, J. Xiao, Y. Tu, D. Deng, H. Yang, H. Tian, J. Li, P. Ren, and X. Bao, "Triggering the electrocatalytic hydrogen evolution activity of the inert two-dimensional MoS_2 surface via single-atom metal doping." *Energy Environ. Sci.*, **8**, 1594 (2015).
156. J. Wang, W. Fang, Y. Hu, Y. Zhang, J. Dang, Y. Wu, B. Chen, H. Zhao, and Z. Li, "Single atom Ru doping 2H-MoS_2 as highly efficient hydrogen evolution reaction electrocatalyst in a wide pH range." *Appl. Catal. B Environ.*, **298**, 120490 (2021).
157. H. Y. Jung, M. J. Chae, J. H. Park, Y. I. Song, J. C. Ro, and S. J. Suh, "Effects of platinum group metals on MoS_2 nanosheets for a high-performance hydrogen evolution reaction catalyst." *ACS Appl. Energy Mater.*, **4**, 10748 (2021).
158. Y. Li, H. Wang, L. Xie, Y. Liang, G. Hong, and H. Dai, "MoS_2 nanoparticles grown on graphene: An advanced catalyst for the hydrogen evolution reaction." *J. Am. Chem. Soc.*, **133**, 7296 (2011).
159. P. Zhang, B. Xu, G. Chen, C. Gao, and M. Gao, "Large-scale synthesis of nitrogen doped MoS_2 quantum dots for efficient hydrogen evolution reaction." *Electrochim. Acta*, **270**, 256 (2018).
160. D. H. Youn, S. Han, J. Y. Kim, J. Y. Kim, H. Park, S. H. Choi, and J. S. Lee, "Highly active and stable hydrogen evolution electrocatalysts based on molybdenum compounds on carbon nanotube-graphene hybrid support." *ACS Nano*, **8**, 5164 (2014).
161. G. Li, J. Huang, Q. Yang, L. Zhang, Q. Mu, Y. Sun, S. Parkin, K. Chang, and C. Felser, "MoS_2 on topological insulator Bi_2Te_3 thin films: activation of the basal plane for hydrogen reduction." *J. Energy Chem.*, **62**, 516 (2021).
162. B. Liu, Y. Cheng, B. Cao, M. Hu, P. Jing, R. Gao, Y. Du, J. Zhang, and J. Liu, "Hybrid heterojunction of molybdenum disulfide/single cobalt atoms anchored nitrogen, sulfur-doped carbon nanotube /cobalt disulfide with multiple active sites for highly efficient hydrogen evolution." *Appl. Catal. B Environ.*, **298**, 120630 (2021).
163. Y. Lv, H. Pan, J. Lin, Z. Chen, Y. Li, H. Li, M. Shi, R. Yin, and S. Zhu, "One-pot hydrothermal approach towards 2D/2D heterostructure based on 1 T MoS_2 chemically bonding with GO for extremely high electrocatalytic performance." *Chem. Eng. J.*, **428**, 132072 (2022).
164. Y. Kumaran, T. Maiyalagan, and S. C. Yi, "An efficient $CoMoS_2$ nanosheets on nitrogen, sulfur dual doped reduced graphene oxide as an electrocatalyst for the hydrogen evolution reaction." *Int. J. Energy Res.*, **45**, 17397 (2021).
165. Z. Lei, S. Xu, and P. Wu, "Ultra-thin and porous $MoSe_2$ nanosheets: facile preparation and enhanced electrocatalytic activity towards the hydrogen evolution reaction." *Phys. Chem. Chem. Phys.*, **18**, 70 (2016).
166. Q. Zhou, G. Zhao, K. Rui, Y. Chen, X. Xu, S. X. Dou, and W. Sun, "Engineering additional edge sites on molybdenum dichalcogenides toward accelerated alkaline hydrogen evolution kinetics." *Nanoscale*, **11**, 717 (2019).
167. X. Xu, W. Xu, L. Zhang, G. Liu, X. Wang, W. Zhong, and Y. Du, "Interface engineering heterostructured MoS_2/WS_2-reduced graphene oxide for enhanced hydrogen evolution electrocatalysts." *Sep. Purif. Technol.*, **278**, 119569 (2022).
168. X. Ji, Y. Lin, J. Zeng, Z. Ren, Z. Lin, Y. Mu, Y. Qiu, and J. Yu, "Graphene/MoS_2/FeCoNi$(OH)_x$ and graphene/MoS_2/FeCoNiPx multilayer-stacked vertical nanosheets on carbon fibers for highly efficient overall water splitting." *Nat. Commun.*, **12**, 1380 (2021).
169. E. P. C. Higgins, A. A. Papaderakis, C. Byrne, R. Cai, A. Elgendy, S. J. Haigh, A. S. Walton, D. J. Lewis, and R. A. W. Dryfe, "High-performance nanostructured MoS_2 electrodes with spontaneous ultralow gold loading for hydrogen evolution." *J. Phys. Chem. C*, **125**, 20940 (2021).
170. J. Ge, D. Zhang, Y. Qin, T. Dou, M. Jiang, F. Zhang, and X. Lei, "Dual-metallic single Ru and Ni atoms decoration of MoS_2 for high-efficiency hydrogen production." *Appl. Catal. B Environ.*, **298**, 120557 (2021).
171. M. Zheng, Q. Chen, and Q. Zhong, "Flower-like 1T-MoS_2/$NiCo_2S_4$ on a carbon cloth substrate as an efficient electrocatalyst for the hydrogen evolution reaction." *Dalt. Trans.*, **50**, 13320 (2021).
172. H.-B. Zheng, Y.-L. Li, Y.-L. Wang, F. Ma, P.-Z. Gao, W.-M. Guo, H. Qin, X.-P. Liu, and H.-N. Xiao, "Fabrication of $Co(PO_3)_2$@NPC/MoS_2 heterostructures for enhanced electrocatalytic hydrogen evolution." *J. Alloys Compd.*, **894**, 162411 (2022).
173. J. Yang, C. Chai, C. Jiang, L. Liu, and J. Xi, "MoS_2–CoS_2 heteronanosheet arrays coated on porous carbon microtube textile for overall water splitting." *J. Power Sources*, **514**, 230580 (2021).
174. A. Muthurasu, V. Maruthapandian, and H. Y. Kim, "Metal-organic framework derived Co_3O_4/MoS_2 heterostructure for efficient bifunctional electrocatalysts for oxygen evolution reaction and hydrogen evolution reaction." *Appl. Catal. B Environ.*, **248**, 202 (2019).
175. D. Cao et al., "Engineering the in-plane structure of metallic phase molybdenum disulfide via Co and O dopants toward efficient alkaline hydrogen evolution." *ACS Nano*, **13**, 11733 (2019).
176. P. Cao, J. Peng, J. Li, and M. Zhai, "Highly conductive carbon black supported amorphous molybdenum disulfide for efficient hydrogen evolution reaction." *J. Power Sources*, **347**, 210 (2017).
177. X. Han, X. Wu, Y. Deng, J. Liu, J. Lu, C. Zhong, and W. Hu, "Ultrafine Pt nanoparticle-decorated pyrite-type CoS_2 nanosheet arrays coated on carbon cloth as a bifunctional electrode for overall water splitting." *Adv. Energy Mater.*, **8**, 1800935 (2018).
178. W. Zhou, D. Hou, Y. Sang, S. Yao, J. Zhou, G. Li, L. Li, H. Liu, and S. Chen, "MoO_2 nanobelts@nitrogen self-doped MoS_2 nanosheets as effective electrocatalysts for hydrogen evolution reaction." *J. Mater. Chem. A*, **2**, 11358 (2014).
179. Y. Deng et al., "Oxygen-incorporated MoX (X: S, Se or P) nanosheets via universal and controlled electrochemical anodic activation for enhanced hydrogen evolution activity." *Nano Energy*, **62**, 338 (2019).
180. Y. Wang, S. Liu, X. Hao, J. Zhou, D. Song, D. Wang, L. Hou, and F. Gao, "Fluorine- and nitrogen-codoped MoS_2 with a catalytically active basal plane." *ACS Appl. Mater. Interfaces*, **9**, 27715 (2017).
181. Y.-J. Tang, Y. Wang, X.-L. Wang, S.-L. Li, W. Huang, L.-Z. Dong, C.-H. Liu, Y.-F. Li, and Y.-Q. Lan, "Molybdenum disulfide/nitrogen-doped reduced graphene oxide nanocomposite with enlarged interlayer spacing for electrocatalytic hydrogen evolution." *Adv. Energy Mater.*, **6**, 1600116 (2016).
182. H. Qian, N. Huang, J. Zheng, Z. An, X. Yin, Y. Liu, W. Yang, and Y. Chen, "A ternary hybrid of Zn-doped MoS_2-RGO for highly effective electrocatalytic hydrogen evolution." *J. Colloid Interface Sci.*, **599**, 100 (2021).
183. K. Wang, Z. Zhan, T. Lei, and P. Yin, "Cu–MoS_2/rGO hybrid material for enhanced hydrogen evolution reaction performance." *Int. J. Hydrogen Energy*, **45**, 9773 (2020).
184. H.-Y. He, "One-step assembly of 2H-1T MoS_2:Cu/reduced graphene oxide nanosheets for highly efficient hydrogen evolution." *Sci Rep.*, **7**, 45608 (2017).
185. F. Li et al., "Synthesis of Cu-MoS_2/rGO hybrid as non-noble metal electrocatalysts for the hydrogen evolution reaction." *J. Power Sources*, **292**, 15 (2015).
186. J. Ma, A. Cai, X. Guan, K. Li, W. Peng, X. Fan, G. Zhang, F. Zhang, and Y. Li, "Preparation of ultrathin molybdenum disulfide dispersed on graphene via cobalt doping: a bifunctional catalyst for hydrogen and oxygen evolution reaction." *Int. J. Hydrogen Energy*, **45**, 9583 (2020).
187. L. X. Chen, Z. W. Chen, Y. Wang, C. C. Yang, and Q. Jiang, "Design of dual-modified MoS_2 with nanoporous Ni and graphene as efficient catalysts for the hydrogen evolution reaction." *ACS Catal.*, **8**, 8107 (2018).
188. X. Xu, W. Zhong, M. Chen, L. Zhang, G. Liu, and Y. Du, "Nanostructural Co–MoS_2/NiCoS supported on reduced graphene oxide as a high activity electrocatalyst for hydrogen evolution in alkaline media." *Int. J. Hydrogen Energy*, **46**, 8567 (2021).
189. A. Pandey, A. Mukherjee, S. Chakrabarty, D. Chanda, and S. Basu, "Interface engineering of an RGO/MoS_2/Pd 2D heterostructure for electrocatalytic overall water splitting in alkaline medium." *ACS Appl. Mater. Interfaces*, **11**, 42094 (2019).
190. Z. Gao, M. Li, J. Wang, J. Zhu, X. Zhao, H. Huang, J. Zhang, Y. Wu, Y. Fu, and X. Wang, "Pt nanocrystals grown on three-dimensional architectures made from graphene and MoS_2 nanosheets: highly efficient multifunctional electrocatalysts toward hydrogen evolution and methanol oxidation reactions." *Carbon N.Y.*, **139**, 369 (2018).
191. Y. Cai, X. Yang, T. Liang, L. Dai, L. Ma, G. Huang, W. Chen, H. Chen, H. Su, and M. Xu, "Easy incorporation of single-walled carbon nanotubes into two-dimensional MoS_2 for high-performance hydrogen evolution." *Nanotechnology*, **25**, 465401 (2014).
192. T. Dong, X. Zhang, P. Wang, H.-S. Chen, and P. Yang, "Formation of Ni-doped MoS_2 nanosheets on N-doped carbon nanotubes towards superior hydrogen evolution." *Electrochim. Acta*, **338**, 135885 (2020).
193. H. Yu, X. Yu, Y. Chen, S. Zhang, P. Gao, and C. Li, "A strategy to synergistically increase the number of active edge sites and the conductivity of MoS_2 nanosheets for hydrogen evolution." *Nanoscale*, **7**, 8731 (2015).
194. X. Guo, G.-L. Cao, F. Ding, X. Li, S. Zhen, Y.-F. Xue, Y.-M. Yan, T. Liu, and K.-N. Sun, "A bulky and flexible electrocatalyst for efficient hydrogen evolution based on the growth of MoS_2 nanoparticles on carbon nanofiber foam." *J. Mater. Chem. A*, **3**, 5041 (2015).
195. N. Xue and P. Diao, "Composite of few-layered MoS_2 grown on carbon black: tuning the ratio of terminal to total sulfur in MoS_2 for hydrogen evolution reaction." *J. Phys. Chem. C*, **121**, 14413 (2017).
196. Y. Wei, Y. Lv, B. Guo, and J. Gong, "Hierarchical molybdenum disulfide nanosheet arrays stemmed from nickel-cobalt layered double hydroxide/carbon cloth for highly-efficient hydrogen evolution reaction." *J. Energy Chem.*, **57**, 587 (2021).
197. P. Xiong et al., "Interface modulation of two-dimensional superlattices for efficient overall water splitting." *Nano Lett.*, **19**, 4518 (2019).
198. F. Yang, Z.-F. Cao, J. Wang, S. Wang, and H. Zhong, "Novel preparation of high activity 1T-phase MoS_2 ultra-thin flakes by layered double hydroxide for enhanced hydrogen evolution performance." *Int. J. Hydrogen Energy*, **44**, 21229 (2019).
199. S. Hussain, I. Rabani, D. Vikraman, T. Mehran, F. Shahzad, Y.-S. Seo, H.-S. Kim, and J. Jung, "Designing the MXene/molybdenum diselenide hybrid nanostructures for high-performance symmetric supercapacitor and hydrogen evolution applications." *Int. J. Energy Res.*, **45**, 18770 (2021).
200. C. Tsai, K. Chan, F. Abild-Pedersen, and J. K. Nørskov, "Active edge sites in $MoSe_2$ and WSe_2 catalysts for the hydrogen evolution reaction: a density functional study." *Phys. Chem. Chem. Phys.*, **16**, 13156 (2014).
201. H. Tang, K. Dou, C.-C. Kaun, Q. Kuang, and S. Yang, "$MoSe_2$ nanosheets and their graphene hybrids: synthesis, characterization and hydrogen evolution reaction studies." *J. Mater. Chem. A*, **2**, 360 (2014).
202. A. Y. S. Eng, A. Ambrosi, Z. Sofer, P. Šimek, and M. Pumera, "Electrochemistry of transition metal dichalcogenides: Strong dependence on the metal-to-chalcogen composition and exfoliation method." *ACS Nano*, **8**, 12185 (2014).
203. Z. Gholamvand et al., "Comparison of liquid exfoliated transition metal dichalcogenides reveals $MoSe_2$ to be the most effective hydrogen evolution catalyst." *Nanoscale*, **8**, 5737 (2016).
204. J. Huang, Y. Jiang, T. Meng, L. Li, and M. Cao, "Regulating electronic structure and adsorptivity in molybdenum selenide for boosting electrocatalytic water splitting." *Electrochim. Acta*, **390**, 138888 (2021).

205. Y. Zhang, S. Zhang, Y. He, H. Li, T. He, H. Shi, X. Ma, Q. Yang, L. Chen, and J. Chen, "Self-supporting $MoSe_2/CoSe_2$@CFP electrocatalyst electrode for high-efficiency HER under alkaline solution." *J. Solid State Chem.*, **298**, 122108 (2021).
206. H. Shu, D. Zhou, F. Li, D. Cao, and X. Chen, "Defect engineering in $MoSe_2$ for the hydrogen evolution reaction: From point defects to edges." *ACS Appl. Mater. Interfaces*, **9**, 42688 (2017).
207. Y. Yao, C. Liu, L. Luo, D. Ji, W. Wang, and Z. Chen, "Microwave hydrothermal synthesis of hierarchical Ce-doped $MoSe_2$@CNTs as an efficient non-precious catalyst for hydrogen evolution in both acidic and alkaline media." *Mater. Res. Bull.*, **146**, 111625 (2022).
208. M. Zhu et al., "Construction of reduced graphene oxide coupled with $CoSe_2$-$MoSe_2$ heterostructure for enhanced electrocatalytic hydrogen production." *J. Colloid Interface Sci.*, **608**, 922 (2022).
209. Y. Tan, M. Yi, Z. Zhu, X. Zhang, K. Qin, J. Zhang, and R. Zhu, "Carbon-coated $MoSe_2/Mo_2CT_x$ (MXene) heterostructure for efficient hydrogen evolution." *Mater. Sci. Eng. B Solid-State Mater. Adv. Technol.*, **271**, 115239 (2021).
210. Z. Shao, L. Wu, H. Ye, X. Ma, X. Zhang, and L. Li, "Promoting effect of MXenes on 1T/2H-$MoSe_2$ for hydrogen evolution." *Cryst. Eng. Comm.*, **23**, 4752 (2021).
211. Z. Guo, Y. Zhao, H. Shi, X. Yuan, W. Zhen, L. He, H. Che, C. Xue, and J. Mu, "$MoSe_2$/g-C_3N_4 heterojunction coupled with Pt nanoparticles for enhanced photocatalytic hydrogen evolution." *J. Phys. Chem. Solids*, **156**, 110137 (2021).
212. C. Tan et al., "Preparation of high-percentage 1T-phase transition metal dichalcogenide nanodots for electrochemical hydrogen evolution." *Adv. Mater.*, **30**, 1705509 (2018).
213. Y. Chen et al., "Coupled heterostructure of Mo-Fe selenide nanosheets supported on carbon paper as an integrated electrocatalyst for efficient hydrogen evolution." *ACS Appl. Mater. Interfaces*, **10**, 27787 (2018).
214. L. Zhang, T. Wang, L. Sun, Y. Sun, T. Hu, K. Xu, and F. Ma, "Hydrothermal synthesis of 3D hierarchical $MoSe_2/NiSe_2$ composite nanowires on carbon fiber paper and their enhanced electrocatalytic activity for the hydrogen evolution reaction." *J. Mater. Chem. A*, **5**, 19752 (2017).
215. K. Zhang, P. P. Jiang, Z. Nie, Q. Gu, and P. Zhang, "Rational design of $MoSe_2$-rGO-CNTs flower-like heterostructures for efficient acidic hydrogen evolution." *J. Solid State Electrochem.*, **25**, 1825 (2021).
216. H. Shi, H. Zhang, M. Li, Y. Wang, and D. Wang, "Nanoflower-like 1T/2H mixed-phase $MoSe_2$ as an efficient electrocatalyst for hydrogen evolution." *J. Alloys Compd.*, **878**, 160381 (2021).
217. S. Deng et al., "Directional construction of vertical nitrogen-doped 1T-2H $MoSe_2$/graphene shell/core nanoflake arrays for efficient hydrogen evolution reaction." *Adv. Mater.*, **29**, 1700748 (2017).
218. M. Zhu, X. Bai, Q. Yan, Y. Yan, K. Zhu, K. Ye, J. Yan, D. Cao, X. Huang, and G. Wang, "Iron molybdenum selenide supported on reduced graphene oxide as an efficient hydrogen electrocatalyst in acidic and alkaline media." *J. Colloid Interface Sci.*, **602**, 384 (2021).
219. N. K. Oh, J. Seo, S. Lee, H.-J. Kim, U. Kim, J. Lee, Y.-K. Han, and H. Park, "Highly efficient and robust noble-metal free bifunctional water electrolysis catalyst achieved via complementary charge transfer." *Nat. Commun.*, **12**, 4606 (2021).
220. M. S. Hassan, P. Basera, S. Gahlawat, P. P. Ingole, S. Bhattacharya, and S. Sapra, "Understanding the efficient electrocatalytic activities of $MoSe_2$-Cu_2S nanoheterostructures." *J. Mater. Chem. A*, **9**, 9837 (2021).
221. A. Dymerska, W. Kukułka, K. Wenelska, and E. Mijowska, "Two-dimensional molybdenum diselenide tuned by bimetal Co/Ni nanoparticles for oxygen evolution reaction." *ACS Omega*, **5**, 28730 (2020).
222. Y. Zhang, C. Zhang, Y. Guo, D. Liu, Y. Yu, and B. Zhang, "Selenium vacancy-rich $CoSe_2$ ultrathin nanomeshes with abundant active sites for electrocatalytic oxygen evolution." *J. Mater. Chem. A*, **7**, 2536 (2019).
223. C. Yu, Z. Cao, S. Chen, S. Wang, H. Zhong, and X. Ma, "In situ selenylation of molybdate ion intercalated Co-Al layered double hydrotalcite for high-performance electrocatalytic oxygen evolution reaction." *J. Taiwan Inst. Chem. Eng.*, **119**, 166 (2021).
224. Y.-J. Tang, Y. Wang, and K. Zhou, "In situ oxidation transformation of trimetallic selenide to amorphous FeCo-oxyhydroxide by self-sacrificing $MoSe_2$ for efficient water oxidation." *J. Mater. Chem. A*, **8**, 7925 (2020).
225. U. De Silva, J. See, W. P. R. Liyanage, J. Masud, J. Wu, W. Yang, W.-T. Chen, D. Prendergast, and M. Nath, "Understanding the structural evolution of a nickel chalcogenide electrocatalyst surface for water oxidation." *Energy Fuels*, **35**, 4387 (2021).
226. Z. Wang, A. Von Dem Bussche, Y. Qiu, T. M. Valentin, K. Gion, A. B. Kane, and R. H. Hurt, "Chemical dissolution pathways of MoS_2 nanosheets in biological and environmental media." *Environ. Sci. Technol.*, **50**, 7208 (2016).
227. S. Chen, C. Yu, Z. Cao, X. Huang, S. Wang, and H. Zhong, "Trimetallic NiFeCr-LDH/MoS_2 composites as novel electrocatalyst for OER." *Int. J. Hydrogen Energy*, **46**, 7037 (2021).
228. M. Rong, F. Yang, C. Yu, S. Wang, H. Zhong, and Z. Cao, "MoS_2/CoAl-LDH heterostructure for enhanced efficient of oxygen evolution reaction." *Colloids Surfaces A Physicochem. Eng. Asp.*, **607**, 125419 (2020).
229. M. Rong, Y. Mo, S. Zhou, X. Ma, S. Wang, Z. Cao, and H. Zhong, "Ce and MoS_2 dual-doped cobalt aluminum layered double hydroxides for enhanced oxygen evolution reaction." *Int. J. Hydrogen Energy*, **47**, 1644 (2022).
230. M. S. Islam, M. Kim, X. Jin, S. M. Oh, N.-S. Lee, H. Kim, and S.-J. Hwang, "Bifunctional 2D Superlattice electrocatalysts of layered double hydroxide-transition metal dichalcogenide active for overall water splitting." *ACS Energy Lett.*, **3**, 952 (2018).
231. J. Cai, X. Zhang, Y. Pan, Y. Kong, and S. Lin, "MoS_2||CoP heterostructure loaded on N, P-doped carbon as an efficient trifunctional catalyst for oxygen reduction, oxygen evolution, and hydrogen evolution reaction." *Int. J. Hydrogen Energy*, **46**, 34252 (2021).
232. X. Tan, Z. Duan, H. Liu, X. Wu, and Y.-R. Cho, "Core-shell structured MoS_2/Ni_9S_8 electrocatalysts for high performance hydrogen and oxygen evolution reactions." *Mater. Res. Bull.*, **146**, 111626 (2022).
233. Y. Yang, K. Zhang, H. Lin, X. Li, H. C. Chan, L. Yang, and Q. Gao, "MoS_2-Ni_3S_2 heteronanorods as efficient and stable bifunctional electrocatalysts for overall water splitting." *ACS Catal.*, **7**, 2357 (2017).
234. Y. Wu et al., "Coupling interface constructions of $MoS_2/Fe_5Ni_4S_8$ heterostructures for efficient electrochemical water splitting." *Adv. Mater.*, **30**, 1803151 (2018).
235. P. Kuang, M. He, H. Zou, J. Yu, and K. Fan, "0D/3D MoS_2-NiS_2/N-doped graphene foam composite for efficient overall water splitting." *Appl. Catal. B Environ.*, **254**, 15 (2019).
236. C. Wang, X. Shao, J. Pan, J. Hu, and X. Xu, "Redox bifunctional activities with optical gain of Ni_3S_2 nanosheets edged with MoS_2 for overall water splitting." *Appl. Catal. B Environ.*, **268**, 118435 (2020).
237. M. Zheng, K. Guo, W.-J. Jiang, T. Tang, X. Wang, P. Zhou, J. Du, Y. Zhao, C. Xu, and J.-S. Hu, "When MoS_2 meets FeOOH: a 'one-stone-two-birds' heterostructure as a bifunctional electrocatalyst for efficient alkaline water splitting." *Appl. Catal. B Environ.*, **244**, 1004 (2019).
238. Y. Yang et al., "Hierarchical nanoassembly of $MoS_2/Co_9S_8/Ni_3S_2$/Ni as a highly efficient electrocatalyst for overall water splitting in a wide pH range." *J. Am. Chem. Soc.*, **141**, 10417 (2019).
239. A. Maiti and S. K. Srivastava, "Ru-Doped CuO/MoS_2 nanostructures as bifunctional water-splitting electrocatalysts in alkaline media, ACS Appl." *Nano Mater.*, **4**, 7675 (2021).
240. Q. Xiong, X. Zhang, H. Wang, G. Liu, G. Wang, H. Zhang, and H. Zhao, "One-step synthesis of cobalt-doped MoS_2 nanosheets as bifunctional electrocatalysts for overall water splitting under both acidic and alkaline conditions." *Chem. Commun.*, **54**, 3859 (2018).
241. B. Tang, Z. G. Yu, H. L. Seng, N. Zhang, X. Liu, Y.-W. Zhang, W. Yang, and H. Gong, "Simultaneous edge and electronic control of MoS_2 nanosheets through Fe doping for an efficient oxygen evolution reaction." *Nanoscale*, **10**, 20113 (2018).
242. C. Santoro, A. Lavacchi, P. Mustarelli, V. Di Noto, L. Elbaz, D. R. Dekel, and F. Jaouen, "What is next in anion-exchange membrane water electrolyzers ? Bottlenecks, benefits, and future." *ChemSusChem*, **15**, e202200027 (2022).
243. V. Ganesan and J. Kim, "Multi-shelled CoS_2–MoS_2 hollow spheres as efficient bifunctional electrocatalysts for overall water splitting." *Int. J. Hydrogen Energy*, **45**, 13290 (2020).
244. Y. Xu, X. Chai, T. Ren, H. Yu, S. Yin, Z. Wang, X. Li, L. Wang, and H. Wang, "Synergism of interface and electronic effects: bifunctional N-doped Ni_3S_2/N-doped MoS_2 hetero-nanowires for efficient electrocatalytic overall water splitting." *Chem. - A Eur. J.*, **25**, 16074 (2019).
245. G. Zhou, X. Wu, M. Zhao, H. Pang, L. Xu, J. Yang, and Y. Tang, "Interfacial engineering-triggered bifunctionality of CoS_2/MoS_2 nanocubes/nanosheet arrays for high-efficiency overall water splitting." *ChemSusChem*, **14**, 699 (2021).
246. J. Hou, B. Zhang, Z. Li, S. Cao, Y. Sun, Y. Wu, Z. Gao, and L. Sun, "Vertically aligned oxygenated-CoS_2-MoS_2 heteronanosheet architecture from polyoxometalate for efficient and stable overall water splitting." *ACS Catal.*, **8**, 4612 (2018).
247. N. Karikalan, P. Sundaresan, S.-M. Chen, R. Karthik, and C. Karuppiah, "Cobalt molybdenum sulfide decorated with highly conductive sulfur-doped carbon as an electrocatalyst for the enhanced activity of hydrogen evolution reaction." *Int. J. Hydrogen Energy*, **44**, 9164 (2019).
248. Y. Hu, H. Yu, L. Qi, J. Dong, P. Yan, T. Taylor Isimjan, and X. Yang, "Interface engineering of needle-like P-doped MoS_2/CoP Arrays as highly active and durable bifunctional electrocatalyst for overall water splitting." *ChemSusChem*, **14**, 1565 (2021).
249. Y. Li, X. Wu, J. Wang, H. Wei, S. Zhang, S. Zhu, Z. Li, S. Wu, H. Jiang, and Y. Liang, "Sandwich structured Ni_3S_2-MoS_2-Ni_3S_2@Ni foam electrode as a stable bifunctional electrocatalyst for highly sustained overall seawater splitting." *Electrochim. Acta*, **390**, 138833 (2021).
250. J.-Y. Xue, F.-L. Li, Z.-Y. Zhao, C. Li, C.-Y. Ni, H.-W. Gu, D. J. Young, and J.-P. Lang, "In situ generation of bifunctional Fe-Doped MoS_2 nanocanopies for efficient electrocatalytic water splitting." *Inorg. Chem.*, **58**, 11202 (2019).
251. S. Song, Y. Wang, W. Li, P. Tian, S. Zhou, H. Gao, X. Tian, and J. Zang, "Amorphous MoS_2 coated $N_{i3}S_2$ nanosheets as bifunctional electrocatalysts for high-efficiency overall water splitting." *Electrochim. Acta*, **332**, 135454 (2020).
252. S. Guan, X. Fu, Z. Lao, C. Jin, and Z. Peng, "NiS-MoS_2 hetero-nanosheet array electrocatalysts for efficient overall water splitting." *Sustain. Energy Fuels*, **3**, 2056 (2019).
253. Z. Yin, X. Liu, S. Chen, H. Xie, L. Gao, A. Liu, T. Ma, and Y. Li, "Interface engineering of the $MoS_2/NiS_2/CoS_2$ nanotube as a highly efficient bifunctional electrocatalyst for overall water splitting." *Mater. Today Nano*, **17**, 100156 (2022).
254. T. Ilyas, F. Raziq, S. Ali, A. Zada, N. Ilyas, R. Shaha, Y. Wang, and L. Qiao, "Facile synthesis of MoS_2/Cu as trifunctional catalyst for electrochemical overall water splitting and photocatalytic CO_2 conversion." *Mater. Des.*, **204**, 109674 (2021).
255. C. Qin, A. Fan, X. Zhang, S. Wang, X. Yuan, and X. Dai, "Interface engineering: few-layer MoS_2 coupled to a NiCo-sulfide nanosheet heterostructure as a bifunctional electrocatalyst for overall water splitting." *J. Mater. Chem. A*, **7**, 27594 (2019).
256. M. Zheng, J. Du, B. Hou, and C.-L. Xu, "Few-Layered $Mo_{(1-x)}W_xS_2$ hollow nanospheres on Ni_3S_2 nanorod heterostructure as robust electrocatalysts for overall water splitting." *ACS Appl. Mater. Interfaces*, **9**, 26066 (2017).

257. L. Guo, Q. Liu, Y. Liu, Z. Chen, Y. Jiang, H. Jin, T. Zhou, J. Yang, and Y. Liu, "Self-supported tremella-like MoS_2-AB particles on nickel foam as bifunctional electrocatalysts for overall water splitting." *Nano Energy*, **92**, 106707 (2022).
258. T. Yoon and K. S. Kim, "One-Step Synthesis of CoS-Doped β-$Co(OH)_2$@Amorphous MoS_{2+x} hybrid catalyst grown on nickel foam for high-performance electrochemical overall water splitting." *Adv. Funct. Mater.*, **26**, 7386 (2016).
259. N. Li, Y. Zhang, M. Jia, X. Lv, X. Li, R. Li, X. Ding, Y.-Z. Zheng, and X. Tao, "1T/2H $MoSe_2$-on-MXene heterostructure as bifunctional electrocatalyst for efficient overall water splitting." *Electrochim. Acta*, **326**, 134976 (2019).
260. G. Janani, S. Yuvaraj, S. Surendran, Y. Chae, Y. Sim, S.-J. Song, W. Park, M.-J. Kim, and U. Sim, "Enhanced bifunctional electrocatalytic activity of Ni-Co bimetallic chalcogenides for efficient water-splitting application." *J. Alloys Compd.*, **846**, 156389 (2020).
261. J. Huang et al., "Multiphase Ni-Fe-selenide nanosheets for highly-efficient and ultra-stable water electrolysis." *Appl. Catal. B Environ.*, **277**, 119220 (2020).
262. Z. Chen, Y. Ha, Y. Liu, H. Wang, H. Yang, H. Xu, Y. Li, and R. Wu, "In situ formation of cobalt ntrides/graphitic carbon composites as efficient bifunctional electrocatalysts for overall water splitting." *ACS Appl. Mater. Interfaces*, **10**, 7134 (2018).
263. J. Mo, S. Wu, T. H. M. Lau, R. Kato, K. Suenaga, T.-S. Wu, Y.-L. Soo, J. S. Foord, and S. C. E. Tsang, "Transition metal atom–doped monolayer MoS_2 in a proton-exchange membrane electrolyzer." *Mater. Today Adv.*, **6**, 100020 (2020).
264. S. Q.-U.-A. Naqvi, S. A. Raza, Y. W. Soon, Y. Liu, J. R. Jennings, and A. New, "WO_3/$FeVO_4$ nanostructured heterojunction for solar-driven water oxidation." *IOP Conf. Ser. Earth Environ. Sci*, **813**, 012011 (2021).
265. C. Lo Vecchio, S. Trocino, G. Giacoppo, O. Barbera, V. Baglio, M. I. Díez-García, M. Contreras, R. Gómez, and A. S. Aricò, "Water splitting with enhanced efficiency using a nickel-based co-catalyst at a cupric oxide photocathode." *Catalysts*, **11**, 1363 (2021).
266. S. Seo et al., "Direct in situ growth of centimeters-cale multi-heterojunction MoS_2/WS_2/WSe_2 thin-film catalyst for photo-electrochemical hydrogen evolution." *Adv. Sci.*, **6**, 1900301 (2019).
267. I. H. Kwak, I. S. Kwon, J. H. Lee, Y. R. Lim, and J. Park, "Chalcogen-vacancy group VI transition metal dichalcogenide nanosheets for electrochemical and photoelectrochemical hydrogen evolution." *J. Mater. Chem. C*, **9**, 101 (2021).
268. N. N. Rosman, R. Mohamad Yunus, L. Jeffery Minggu, K. Arifin, M. B. Kassim, and M. A. Mohamed, "Vertical MoS_2 on SiO_2/Si and graphene: effect of surface morphology on photoelectrochemical properties." *Nanotechnology*, **32**, 035705 (2021).
269. Q. Ding, F. Meng, C. R. English, M. Cabán-Acevedo, M. J. Shearer, D. Liang, A. S. Daniel, R. J. Hamers, and S. Jin, "Efficient photoelectrochemical hydrogen generation using heterostructures of Si and chemically exfoliated metallic MoS_2." *J. Am. Chem. Soc.*, **136**, 8504 (2014).
270. K. K. Paul, N. Sreekanth, R. K. Biroju, T. N. Narayanan, and P. K. Giri, "Solar light driven photoelectrocatalytic hydrogen evolution and dye degradation by metal-free few-layer MoS_2 nanoflower/TiO_2(B) nanobelts heterostructure." *Sol. Energy Mater. Sol. Cells*, **185**, 364 (2018).
271. X. Ren, X. Qi, Y. Shen, S. Xiao, G. Xu, Z. Zhang, Z. Huang, and J. Zhong, "2D co-catalytic MoS_2 nanosheets embedded with 1D TiO_2 nanoparticles for enhancing photocatalytic activity." *J. Phys. D: Appl. Phys.*, **49**, 315304 (2016).
272. X. Liu, Z. Xing, Y. Zhang, Z. Li, X. Wu, S. Tan, X. Yu, Q. Zhu, and W. Zhou, "Fabrication of 3D flower-like black N-TiO_{2-x}@MoS_2 for unprecedented-high visible-light-driven photocatalytic performance." *Appl. Catal. B Environ.*, **201**, 119 (2017).
273. L. Ye, H. Zhang, Y. Xiong, C. Kong, H. Li, and W. Li, "Efficient photoelectrochemical overall water-splitting of MoS_2/g-C_3N_4 n-n type heterojunction film." *J. Chem. Phys.*, **154**, 214701 (2021).
274. Z. Masoumi, M. Tayebi, M. Kolaei, and B.-K. Lee, "Unified surface modification by double heterojunction of MoS_2 nanosheets and $BiVO_4$ nanoparticles to enhance the photoelectrochemical water splitting of hematite photoanode." *J. Alloys Compd.*, **890**, 161802 (2022).
275. C. Liu, B. Chai, C. Wang, J. Yan, and Z. Ren, "Solvothermal fabrication of MoS_2 anchored on $ZnIn_2S_4$ microspheres with boosted photocatalytic hydrogen evolution activity." *Int. J. Hydrogen Energy*, **43**, 6977 (2018).
276. J. E. Samaniego-Benitez, L. Lartundo-Rojas, A. García-García, H. A. Calderón, and A. Mantilla, "One-step synthesis and photocatalytic behavior for H_2 production from water of ZnS/MoS_2 composite material." *Catal. Today*, **360**, 99 (2021).
277. S. Tiwari, S. Kumar, and A. K. Ganguli, "Role of MoS_2/rGO co-catalyst to enhance the activity and stability of Cu_2O as photocatalyst towards photoelectrochemical water splitting." *J. Photochem. Photobiol. A Chem.*, **424**, 113622 (2022).
278. Y. Liu, Y.-X. Yu, and W.-D. Zhang, "MoS_2/CdS heterojunction with high photoelectrochemical activity for H_2 evolution under visible light: the role of MoS_2." *J. Phys. Chem. C*, **117**, 12949 (2013).
279. T. A. Ho, C. Bae, J. Joe, H. Yang, S. Kim, J. H. Park, and H. Shin, "Heterojunction photoanode of atomic-layer-deposited MoS_2 on single-crystalline CdS nanorod arrays." *ACS Appl. Mater. Interfaces*, **11**, 37586 (2019).
280. S. Vanka, Y. Wang, P. Ghamari, S. Chu, A. Pandey, P. Bhattacharya, I. Shih, Z. Mi, and A. High, "Efficiency Si photoanode protected by few-layer $MoSe_2$." *Sol. RRL*, **2**, 1800113 (2018).
281. G. Huang, J. Mao, R. Fan, Z. Yin, X. Wu, J. Jie, Z. Kang, and M. Shen, "Integrated $MoSe_2$ with n+p-Si photocathodes for solar water splitting with high efficiency and stability." *Appl. Phys. Lett.*, **112**, 013902 (2018).
282. M. Ben-Naim et al., "Addressing the stability gap in photoelectrochemistry: Molybdenum disulfide protective catalysts for tandem III-V unassisted solar water splitting." *ACS Energy Lett.*, **5**, 2631 (2020).
283. K. R. G. Lim, A. D. Handoko, L. R. Johnson, X. Meng, M. Lin, G. S. Subramanian, B. Anasori, Y. Gogotsi, A. Vojvodic, and Z. W. Seh, "2H-MoS_2 on Mo_2CT_x MXene nanohybrid for efficient and durable electrocatalytic hydrogen evolution." *ACS Nano.*, **14**, 16140 (2020).
284. A.-Y. Lu et al., "Janus monolayers of transition metal dichalcogenides." *Nat. Nanotechnol.*, **12**, 744 (2017).
285. J. Zhang et al., "Janus monolayer transition-metal dichalcogenides." *ACS Nano*, **11**, 8192 (2017).
286. X. Lei, C. Ouyang, and K. Huang, "A first-principles investigation of Janus MoSSe as a catalyst for photocatalytic water-splitting." *Appl. Surf. Sci.*, **537**, 147919 (2021).
287. G. Wang, C. Chen, B. S. Teketel, B. Xu, and B. Lin, "Constructing a new 2D Janus black phosphorus/SMoSe heterostructure for spontaneous wide-spectral-responsive photocatalytic overall water splitting." *Int. J. Hydrogen Energy*, **46**, 39183 (2021).
288. X. Ma, X. Yong, C.-C. Jian, and J. Zhang, "Transition metal-functionalized Janus MoSSe monolayer: a magnetic and efficient single-atom photocatalyst for water-splitting applications." *J. Phys. Chem. C*, **123**, 18347 (2019).
289. S. Wei, J. Li, X. Liao, H. Jin, and Y. Wei, "Investigation of stacking effects of bilayer MoSSe on photocatalytic water splitting." *J. Phys. Chem. C*, **123**, 22570 (2019).
290. Z. Wang, C. Li, and K. Domen, "Recent developments in heterogeneous photocatalysts for solar-driven overall water splitting." *Chem. Soc. Rev.*, **48**, 2109 (2019).